30 Ahmad I, Dooley CM, Thoreson WB et al. In vitro analysis of a mammalian retinal progenitor that gives rise to neurons and glia. Brain Res 1999;831:1–10.

31 Tropepe V, Coles BL, Chiasson BJ et al. Retinal stem cells in the adult mammalian eye. Science 2000;287:2032–2036.

32 Klassen HJ, Ng TF, Kurimoto Y et al. Multipotent retinal progenitors express developmental markers, differentiate into retinal neurons, and preserve light-mediated behavior. Invest Ophthalmol Vis Sci 2004;45: 4167–4173.

33 Yokoyama A, Yang L, Itoh S et al. Microglia, a potential source of neurons, astrocytes, and oligodendrocytes. Glia 2004;45:96–104.

34 Tanaka R, Komine-Kobayashi M, Mochizuki H et al. Migration of enhanced green fluorescent protein expressing bone marrow-derived microglia/macrophage into the mouse brain following permanent focal ischemia. Neuroscience 2003;117:531–539.

35 Eglitis MA, Mezey E. Hematopoietic cells differentiate into both microglia and macroglia in the brains of adult mice. Proc Natl Acad Sci U S A 1997;94:4080–4085.

36 Zhang Y, Caffe AR, Azadi S et al. Neuronal integration in an abutting-retinas culture system. Invest Ophthalmol Vis Sci 2003;44:4936–4946.

37 Zhang Y, Kardaszewska AK, van Veen T et al. Integration between abutting retinas: Role of glial structures and associated molecules at the interface. Invest Ophthalmol Vis Sci 2004;45:4440–4449.

38 Akita J, Takahashi M, Hojo M et al. Neuronal differentiation of adult rat hippocampus-derived neural stem cells transplanted into embryonic rat explanted retinas with retinoic acid pretreatment. Brain Res 2002;954: 286–293.

39 Zahir T, Klassen H, Young MJ. Effects of ciliary neurotrophic factor on differentiation of late retinal progenitor cells. STEM CELLS 2005;23: 424–432.

40 Aggarwal S, Pittenger MF. Human mesenchymal stem cells modulate allogeneic immune cell responses. Blood 2005;105:1815–1822.

41 Beyth S, Borovsky Z, Mevorach D et al. Human mesenchymal stem cells alter antigen-presenting cell maturation and induce T-cell unresponsiveness. Blood 2005;105:2214–2219.

42 Alvarez-Dolado M, Pardal R, Garcia-Verdugo JM et al. Fusion of bone-marrow-derived cells with Purkinje neurons, cardiomyocytes and hepatocytes. Nature 2003;425:968–973.

43 Weimann JM, Johansson CB, Trejo A et al. Stable reprogrammed heterokaryons form spontaneously in Purkinje neurons after bone marrow transplant. Nat Cell Biol 2003;5:959–966.

44 Pochampally RR, Neville BT, Schwarz EJ et al. Rat adult stem cells (marrow stromal cells) engraft and differentiate in chick embryos without evidence of cell fusion. Proc Natl Acad Sci U S A 2004;101:9282–9285.

45 Cogle CR, Yachnis AT, Laywell ED et al. Bone marrow transdifferentiation in brain after transplantation: A retrospective study. Lancet 2004; 363:1432–1437.

46 Tremain N, Korkko J, Ibberson D et al. MicroSAGE analysis of 2,353 expressed genes in a single cell-derived colony of undifferentiated human mesenchymal stem cells reveals mRNAs of multiple cell lineages. STEM CELLS 2001;19:408–418.

47 Seshi B, Kumar S, King D. Multilineage gene expression in human bone marrow stromal cells as evidenced by single-cell microarray analysis. Blood Cells Mol Dis 2003;31:268–285.

48 Woodbury D, Reynolds K, Black IB. Adult bone marrow stromal stem cells express germline, ectodermal, endodermal, and mesodermal genes prior to neurogenesis. J Neurosci Res 2002;69:908–917.

49 Hori J, Ng TF, Shatos M et al. Neural progenitor cells lack immunogenicity and resist destruction as allografts. STEM CELLS 2003; 21:405–416.

50 Klassen H, Imfeld KL, Ray J et al. The immunological properties of adult hippocampal progenitor cells. Vision Res 2003;43:947–956.

Journal of Cellular Biochemistry 100:1240–1254 (2007)

Hyaline Cartilage Formation and Enchondral Ossification Modeled With KUM5 and OP9 Chondroblasts

Tadashi Sugiki,[1,2] Taro Uyama,[1] Masashi Toyoda,[1] Hideo Morioka,[2] Shoen Kume,[3] Kenji Miyado,[1] Kenji Matsumoto,[4] Hirohisa Saito,[4] Noriyuki Tsumaki,[5] Yoriko Takahashi,[6] Yoshiaki Toyama,[2] and Akihiro Umezawa[1]*

[1]Department of Reproductive Biology and Pathology, National Institute for Child and Health Development, Tokyo 157-8535, Japan
[2]Department of Orthopaedic Surgery, Keio University School of Medicine, Tokyo 160-8582, Japan
[3]Division of Stem Cell Biology, Department of Regeneration Medicine, Institute of Molecular Embryology and Genetics, Kumamoto University, Kuhonji, Kumamoto 862-0976, Japan
[4]Department of Allergy & Immunology, National Research Institute for Child Health and Development, Tokyo, Japan
[5]Department of Orthopaedics, Osaka University Graduate School of Medicine, 2-2 Yamadaoka, Suita, Osaka 565-0871, Japan
[6]Mitsui Knowledge Industry, Co, Ltd, Harmony Tower 21st Floor, 1-32-2 Honcho, Nakano-ku, Tokyo 164-8721, Japan

Abstract What is it that defines a bone marrow-derived chondrocyte? We attempted to identify marrow-derived cells with chondrogenic nature and immortality without transformation, defining "immortality" simply as indefinite cell division. KUM5 mesenchymal cells, a marrow stromal cell line, generated hyaline cartilage in vivo and exhibited enchondral ossification at a later stage after implantation. Selection of KUM5 chondroblasts based on the activity of the chondrocyte-specific cis-regulatory element of the collagen α2(XI) gene resulted in enhancement of their chondrogenic nature. Gene chip analysis revealed that OP9 cells, another marrow stromal cell line, derived from macrophage colony-stimulating factor-deficient osteopetrotic mice and also known to be niche-constituting cells for hematopoietic stem cells expressed chondrocyte-specific or -associated genes such as type II collagen α1, Sox9, and cartilage oligomeric matrix protein at an extremely high level, as did KUM5 cells. After cultured OP9 micromasses exposed to TGF-β3 and BMP2 were implanted in mice, they produced abundant metachromatic matrix with the toluidine blue stain and formed type II collagen-positive hyaline cartilage within 2 weeks in vivo. Hierarchical clustering and principal component analysis based on microarray data of the expression of cell surface markers and cell-type-specific genes resulted in grouping of KUM5 and OP9 cells into the same subcategory of "chondroblast," that is, a distinct cell type group. We here show that these two cell lines exhibit the unique characteristics of hyaline cartilage formation and enchondral ossification in vitro and in vivo. J. Cell. Biochem. 100: 1240–1254, 2007. © 2006 Wiley-Liss, Inc.

Key words: Hyaline cartilage; chondroblasts; enchondral ossification; bioinformatics; gene chip

This article contains supplementary material, which may be viewed at the Journal of Cellular Biochemistry website at http://www.interscience.wiley.com/jpages/0730-2312/suppmat/index.html.

Grant sponsor: Research on Health Science focusing on Drug Innovation (KH71064) from the Japan Health Science Foundation; Grant sponsor: The program for promotion of fundamental Studies in Health Science of the Pharmaceuticals and Medical Devices Agency (PMDA); Grant sponsor: The Ministry of Education, Culture, Sports, Science, and Technology (MEXT) of Japan; Grant sponsor: The Health, Labour Sciences Research Grants; Grant sponsor: The Pharmaceuticals and Medical Devices Agency; Grant sponsor: The research Grant for Cardiovascular Disease (H16C-6) from the ministry of Health, Labour and Welfare; Grant sponsor: Grant for Child Health and Development (H15C-2) from the Ministry of Health, Labour and Welfare.

*Correspondence to: Akihiro Umezawa, MD, PhD, Department of Reproductive Biology and Pathology, National Research Institute for Child Health and Development, 2-10-1, Okura, Setagaya, Tokyo 157-8535, Japan.
E-mail: umezawa@1985.jukuin.keio.ac.jp

Received 28 March 2006; Accepted 26 July 2006
DOI 10.1002/jcb.21125

The concept of regenerative medicine refers to the cell-mediated restoration of damaged or diseased tissue, and practically, regeneration of bone and cartilage may be one of the most accessible approaches. Candidate cell sources for regeneration of tissue include embryonic stem cells, fetal cells, or adult cells such as marrow stromal cells [Bianco and Robey, 2000], each of which has both benefits and drawbacks. Multipotent mesenchymal stem cells proliferate extensively, and to maintain the ability to differentiate into multiple cell types such as osteoblasts, chondrocytes, cardiomyocytes, adipocytes, and myoblasts in vitro [Umezawa et al., 1992; Pittenger et al., 1999; Bianco and Robey, 2000]. Marrow-derived stromal cells are also able to generate cardiomyocytes and endothelial cells [Makino et al., 1999], neuronal cells [Kohyama et al., 2001], and adipocytes [Umezawa et al., 1991]. Thus, marrow stromal cells are expected to be a good source of cell therapy in addition to embryonic stem cells and fetal cells [Pittenger et al., 1999].

In adults, chondrocytes maintain the extracellular matrix that gives cartilage its unique mechanical properties. Chondrocytes are long-lived and the development of new cells that are capable of producing cartilage de novo (i.e., chondroblasts) is not a normal part of adult cartilage physiology. A better understanding of the molecular mechanisms that regulate postnatal chondroblast differentiation would have a high impact on the design of strategies for cartilage repair. Cultures are commonly made from suspensions of cells dissociated from cartilage. Cartilage-derived cells in primary cultures can be removed from the culture dish and made to proliferate to form a large number of so-called secondary cultures: in this way, these cells may be repeatedly subcultured for weeks or months. Such cells often display many of the differentiated properties appropriate to their origin: the phenotype of the differentiated chondrocyte is characterized by the synthesis, deposition, and maintenance of cartilage-specific extracellular matrix molecules, including type II collagen and aggrecan [Archer et al., 1990; Hauselmann et al., 1994; Reginato et al., 1994]. The phenotype of differentiated chondrocytes is unstable in culture and is rapidly lost during serial monolayer subculturing [Benya and Shaffer, 1982; Lefebvre et al., 1990; Bonaventure et al., 1994]. This process is referred to as "dedifferentiation" and is a major impediment to the use of mass cell populations for cell therapy or tissue engineering of damaged cartilage. However, when cultured three-dimensionally in a scaffold such as agarose, collagen, or alginate, redifferentiated chondrocytes start to reexpress the chondrocytic differentiation phenotype.

This study was undertaken to obtain bone marrow-derived chondroblastic cell lines that retain critical in vivo cell functions. Previous studies showed that it was possible to obtain lines of bone marrow-derived mesenchymal stem cells, mammary gland epithelial cells, skin keratinocytes, and pigmented epithelial cells that retained critical in vivo cell functions. By implanting cells into immunodeficient mice, we identified a newly isolated KUM5 chondroblastic cell line capable of in vivo hyaline-type chondrogenesis and serendipitously found that OP9 cells derived from osteopetrotic mice and also known as a niche-constituting cells for hematopoietic stem cells had chondrogenic potential.

MATERIALS AND METHODS

Cell Culture and Chondrogenic Differentiation

The cells were cultured in the growth medium (GM): Dulbecco's modified Eagle's medium (DMEM) with high glucose supplemented with 10% fetal bovine serum for KUM5 cells; α-MEM supplemented with 10% serum (BIOWEST, lot number: S03400S1820) for OP9 cells. For chondrogenic induction of pellet culture [Johnstone et al., 1998], both KUM5 and OP9 cells were cultured in the chondrogenic medium (CM): DMEM-high glucose containing 0.1 μM dexamethasone, 1 mM sodium pyruvate, 0.17 mM ascorbic acid-2-phosphate, 0.35 mM proline, 6.25 μg/ml bovine insulin, 6.25 μg/ml transferrin, 6.25 μg/ml selenous acid, 5.33 μg/ml linoleic acid, and 1.25 mg/ml BSA (BioWhittaker). In the chondrogenic differentiation, the combination of one or several growth factors was added to the CM: TGF-β3 10 ng/ml, BMP2 50 ng/ml, BMP4 50 ng/ml, BMP6 50 ng/ml, BMP7 50 ng/ml, PDGF 50 ng/ml, hyaluronic acid 250 ng/ml. The cells and the pellets were maintained at 37°C with 5% CO_2.

Scanning Electron Microscopy (SEM) and Transmission Electron Microscopy (TEM)

The pelleted micromasses were examined by SEM and TEM. The micromasses were coated

with gold using a Sputter Coater (Sanyu Denshi Co., Tokyo, Japan) for SEM. The gas pressure was set at 50 mtorr, the current was 5 mA, and the coating time was 180 s. The samples were examined with a scanning electron microscope (JSM-6400Fs; JEOL, Ltd., Tokyo, Japan) operated at a voltage of 3 kV. For TEM, the micromasses and cell implants were initially fixed in PBS containing 2.5% glutaraldehyde for 24 h, and were embedded in epoxy resin. Ultrathin sections were double stained with uranyl acetate and lead citrate and were viewed under a JEM-1200EX transmission electron microscope (JEOL, Ltd.).

Flow Cytometric Analysis

Cells were transfected with p742-Venus-Int plasmid and were cultured for 72 h. Venus-positive cells were sorted using the cell sorter (EPICS ALTRA, Deckman Coulter, Inc., Fullerton, CA).

Preparation and Transfection of Plasmid

The Venus gene (gift from Miyawaki) was obtained by BamHI and NotI digestion of Venus/pCS2 [Nagai et al., 2002]. The Venus gene was then cloned between the BamHI and NotI sites of pBluescriptII SK (−), excised by SalI and NotI digestion, and inserted between the XhoI and NotI sites of the p742-LacZ plasmid [Tsumaki et al., 1996], from which the LacZ gene was excised by XhoI and NotI digestion. This was named p742-Venus-Int plasmid. Transfection was performed using LipofectAmine 2000 (Invitrogen Japan K.K., Tokyo, Japan) according to the manufacturer's instructions.

Isolation of KUM5 Chondroblast

Cells were transfected with p742-Venus-Int plasmid and were cultured for 72 h. Venus-positive cells were sorted using the cell sorter (EPICS ALTRA, Deckman Coulter, Inc., Fullerton, CA).

In Vivo Cell Implantation Assay

To determine the ability of cultured cells to differentiate in vivo, freshly scraped cells ($2–3 \times 10^7$ cells) were subcutaneously inoculated into Balb/c nu/nu mice (Sankyo Laboratory, Hamamatsu, Japan) as previously described [Umezawa et al., 1992]. Animals were sacrificed by cervical dislocation between 1 and 8 weeks after inoculation. The subcutaneous specimens were dissected at various times after implantation and fixed and decalcified for 1 week in 10% EDTA (pH 8.0) solution. After dehydration in ascending concentrations of ethanol and xylene, the implants were embedded in paraffin. The paraffin sections were then deparaffinized, hydrated, and stained with hematoxylin and eosin, alcian blue, or toluidine blue. Paraffin sections were immunohistochemically stained with anti-type II collagen antibodies (Daiichi Fine Chemical Co., Ltd., Tokyo, Japan, Product No. F-57).

All animals received humane care in compliance with the "Principles of Laboratory Animal Care" formulated by the National Society for Medical Research and the "Guide for the Care and Use of Laboratory Animals" prepared by the Institute of Laboratory Animal Resources and published by the US National Institutes of Health (NIH Publication No. 86–23, revised 1985). The operation protocols were accepted by the Laboratory Animal Care and Use Committee of the Research Institute for Child and Health Development (2003–002).

Gene Chip Expression Analysis

Mouse-genome-wide gene expression was examined with the Mouse Genome MOE430A Probe array (GeneChip, Affymetrix), which contains the oligonucleotide probe set for approximately 23,000 full-length genes and expressed sequence tags (ESTs), according to the manufacturer's protocol (Expression Analysis Technical Manual and GeneChip small sample target labeling Assay Version 2 technical note. http://www.affymetrix.com/support/technical/index.affx). Total RNA was isolated with an RNeasy mini-kit (Qiagen, Chatsworth, CA). Double-stranded cDNA was synthesized, and the cDNA was subjected to in vitro transcription in the presence of biotinylated nucleoside triphosphates. The biotinylated cRNA was hybridized with a probe array for 16 h at 45°C, and the hybridized biotinylated cRNA was stained with streptavidin-PE and scanned with a Hewlett–Packard Gene Array Scanner. The fluorescence intensity of each probe was quantified by using the GeneChip Analysis Suite 5.0 computer program (Affymetrix). The expression level of a single mRNA was determined as the average fluorescence intensity among the intensities obtained with 11 paired (perfect matched and single nucleotide-mismatched) probes consisting of 25-mer oligonucleotides. If the intensities of mismatched probes was very high, gene

expression was judged to be absent (A), even if high average fluorescence was obtained with the GeneChip Analysis Suite 5.0 program. The level of gene expression was determined with the GeneChip software as the average difference (AD). Specific AD levels were then calculated as percentages of the mean AD level of six probe sets for housekeeping genes (β-actin and GAPDH). Further data analysis was performed with the Genespring software version 5 (Silicon Genetics, San Carlos, CA). To normalize the staining intensity variations among chips, the AD values for all genes on a given chip were divided by the median of all measurements on that chip. To eliminate changes within the range of background noise and to select the most differentially expressed genes, data were used only if the raw data values were less than 100 AD and gene expression was judged to be present by the Affymetrix data analysis.

Hierarchical Clustering and Principal Component Analysis

To analyze the gene expression data in an unsupervised manner by gene chip array, we used agglomerative hierarchical clustering and principal component analysis (PCA) (http://lgsun.grc.nia.nih.gov/ANOVA/). The hierarchical clustering techniques classify data by similarity and there results are represented by dendrogram. PCA is a multivariate analysis technique which finds major pattern in data variability. Hierarchical clustering and PCA were performed to group mesenchymal cells obtained from bone marrow into subcategories. Expression data of 244 cell surface marker genes (Supplementary Table I), 34 fat-associated genes (Supplementary Table II), 36 cartilage-associated genes (Supplementary Table III) dotted onto the gene chip were used for analysis.

RESULTS

Pelleted Micromass Culture of KUM5 Cells

KUM5 cells, one of the cloned lines of cells, were found to exhibit chondrogenesis in vivo within 4 weeks after direct injection. This possible chondrogenic cell line was subcloned by the limiting dilution method to obtain a cell line capable of forming elastic, fibrous or hyaline cartilage. When cultured in monolayer, KUM5 cells had a fibroblast-like morphology, and their doubling time was approximately 29.7 h. After reaching confluence, the cells had larger nucleus and cytoplasm, and generated so-called "chondrogenic nodules." We performed the micromass culture of KUM5 cells in the GM or the CM, and continued the pelleted micromass culture for up to 10 weeks (Fig. 1A). The cells were equally embedded in the extracellular matrix, and the extracellular matrix of the KUM5 pellet culture did not show metachromasia with toluidine blue staining in the GM and the CM. Since transforming growth factor (TGF)-β and bone morphogeneic protein (BMP) are involved in chodrogenesis and osteogenesis [Fujii et al., 1999; Maeda et al., 2004], we used TGF-β3 and BMPs on KUM5 culture. Exposure of the cells to TGF-β3 augmented the metachromatic toluidine blue staining in the KUM5-micromass (Fig. 1A,B). BMP2 dramatically enhanced this TGF-β3-induced differentiation, that is, caused stronger metachromatic staining and enlarged metachromatic area. To determine the effect of other cytokines on the TGF-β3-induced chondrogenic differentiation, we added BMP4, BMP6, BMP7, PDGF, or hyaluronic acid to the CM supplemented with TGF-β3. BMP4, BMP6, and BMP7 enhanced the TGF-β3-induced chondrogenic differentiation in a manner similar to BMP2 (Fig. 1C,D). With exposure to BMP2, the number of the postmitotic daughter cells in the cell nest increased, matrix became more abundant, and hypertrophic chondrocytes became larger at higher magnification (Fig. 1E). In contrast, PDGF inhibited the TGF-β3 and BMP4-induced differentiation, as determined by toluidine blue staining (Fig. 1Ce,De). To confirm the chondrogenetic differentiation histologically, we examined the ultrastructural analysis of the cartilaginous micromasses. Extracellular matrix was abundantly deposited over KUM5 cells, or the surface of the generated micromass. The cells covering the micromass showed a flattened shape (Fig. 3A,B). The KUM5 chondrocytes inside the micromass showed an oval or round structure, had cellular processes, and were embedded in the hypertrophic chondrocytes. Abundant rough endoplasmic reticulum and a small number of mitochondria were observed in the KUM5 chondrocytes (Fig. 3C).

Gene Chip Analysis of the KUM5 and OP9 Chondroblasts

To clarify the specific gene expression profile of marrow stromal cells, we compared the

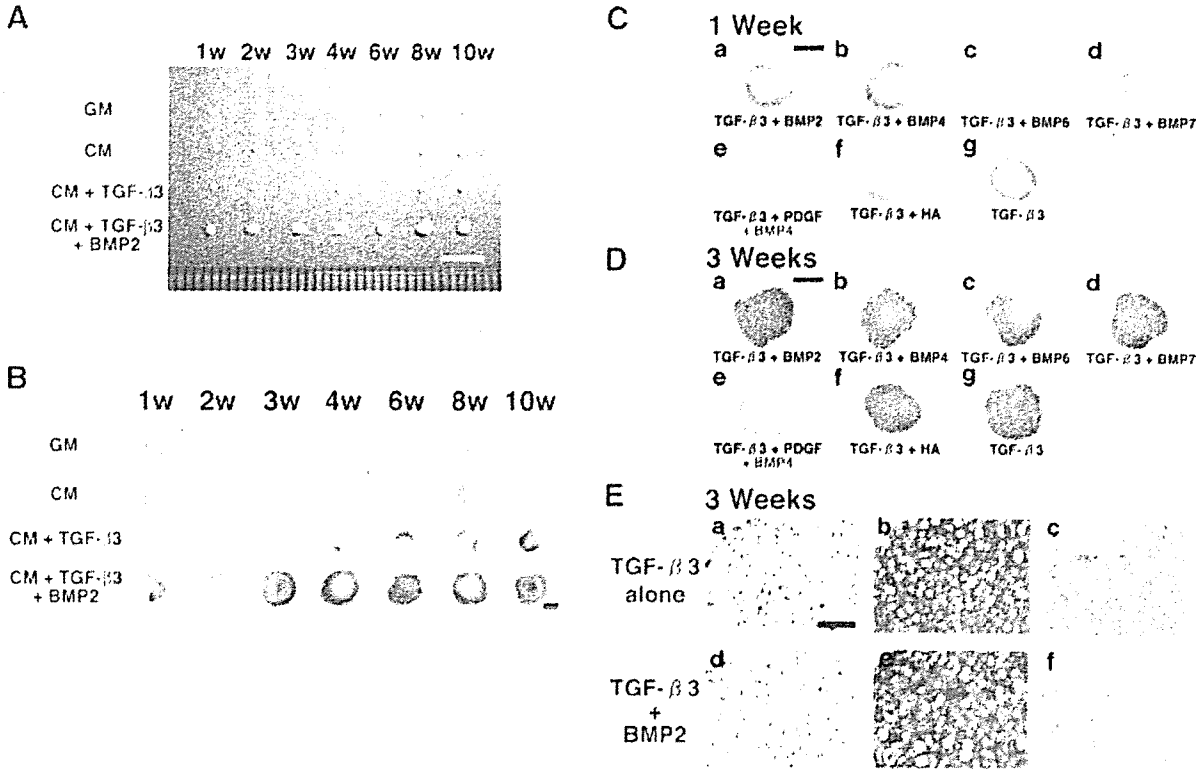

Fig. 1. In vitro chondrogenesis of KUM5 cells. **A,B**: Time-course analysis of growth factors-induced matrix production in KUM5 cells. Macroscopic view of KUM5 chondrogenic nodules which were generated after pellet culture for 1–10 weeks in the GM or the CM supplemented with or without growth factors as indicated (see "Cell culture" Section in Materials and Methods) (A) and toluidine blue stained section (B). BMP2 drastically enhanced TGF-β3-induced matrix production of KUM5 cells. **C,D**: Toluidine blue stained section of KUM5 chondrogenic nodules in the pellet culture exposed to growth factors as indicated for 1 week (C) or 3 weeks (D). **E**: Higher magnification of KUM5 chondrogenic pellet exposed to TGF-β3 (**a**–**c**), or TGF-β3 and BMP2 (**d**–**f**) for 3 weeks. **a,d**: hematoxylin and eosin stain; **b,e**: toluidine blue stain; **c,f**: alcian blue stain. Scale bars: 5 mm (A), 500 μm (B, C, D), 100 μm (E).

expression levels of approximately 23,000 genes in the KUM5, 9-15c, KUSA-O, KUSA-A1, H-1/A, and OP9 cells [Umezawa et al., 1992; Nakano et al., 1994]. (http://1954.jukuin.keio.ac.jp/umezawa/chip/sugiki) by using the Affymetrix gene chip oligonucleotide arrays (Table I). RNAs were isolated from cell lines cultured in the GM without any induction of differentiation to perform the gene chip analysis. Of the 23,000 genes represented on the gene chip, chondrocyte-specific- or associated-genes such as type II collagen α1, Sox9, and cartilage oligomeric matrix protein were more strongly expressed in KUM5 cells than in other marrow-derived mesenchymal cells. Surprisingly, OP9 cells [Nakano, 1996] also expressed these chondrocyte-specific or -associated genes at higher levels: the type II collagen α1, and cartilage oligomeric matrix protein genes were expressed in OP9 cells at more than tenfold higher levels than in 9–15c mesenchymal stem cells, KUSA-O osteo-adipogenic progenitor cells, H-1/A preadipocytes, or even KUM5 chondroblasts. These results implied that KUM5 and OP9 cells have increased chondrogenic potential.

Pelleted Micromass Culture of OP9 Cells

We performed the pellet culture of OP9 cells in the GM and continued the culture for up to 10 weeks (Fig. 2A). The cells were equally embedded in the extracellular matrix and the extracellular matrix of the OP9 pellet culture did not show metachromasie with the toluidine blue stain in the GM (data not shown). With exposure to TGF-β3, the cells in the peripheral zone generated cartilage and exhibited adipocyte-like morphology in the center (Fig. 2Bg,Cg). Next, we investigated the effect of BMP2 in the pellet culture of OP9 cells. The CM with TGF-β3 and BMP2 dramatically induced the chondrogenic differentiation (Fig. 2A,Ba,Ca), that is, the pellet cells produced

TABLE I. Cartilage-Associated Genes Expressed in KUM5 and OP9 Cells in Comparison With Other Marrow Stromal Cells

			9–15c		KUSA-O		KUSA-A1		H-1/A		OP9		KUM5		
Probe set	Genbank	Description	Flags	Raw	Flags	Raw	Flags	Raw	Flags	Raw	Flags	Raw	Flags	Raw	Symbol
1450567_a_at	NM_031163	Procollagen, type II, alpha 1	A	28	A	187	A	98	A	46	P	1,7390	P	679	Col2a1
1428571_at	AK004383	Procollagen, type IX, alpha 1	P	85	P	116	P	99	P	57	P	132	P	190	Col9a1
1422253_at	NM_009925	Procollagen, type X, alpha 1	A	13	A	20	A	15	A	104	A	218	A	270	Col10a1
1418599_at	BB836814	Procollagen, type XI, alpha 1	A	69	P	682	P	4,284	P	5,009	P	2,551	P	518	Col11a1
1419527_at	NM_016685	Cartilage oligomeric matrix protein	A	120	A	111	A	64	A	167	P	1,892	M	172	Comp
1449368_at	NM_007833	Decorin	A	176	A	36	A	223	A	226	A	85	A	110	Dcn
1416405_at	BC019502	Biglycan	P	12,600	P	11,817	P	11,011	P	12,932	P	21,954	P	18,640	Bgn
1449827_at	NM_007424	Aggrecan 1	A	70	A	118	A	105	A	127	A	94	A	167	Agc1
1416321_s_at	BC019775	Proline arginine-rich end leucine-rich repeat	P	196	A	59	P	899	P	1,092	P	2,169	P	362	Prelp
1415939_at	NM_021355	Fibromodulin	P	388	M	359	P	11,542	P	16,626	A	108	A	320	Fmod
1418745_at	NM_012050	Osteomodulin	P	288	A	50	P	1,849	P	2,185	P	347	P	743	Omd
1415943_at	BC010560	Syndecan 1	P	1,182	P	2,449	P	1,358	P	1,607	P	4,704	P	1,799	Sdc1
1417012_at	AI266824	Syndecan 2	P	752	P	1,256	P	2,940	P	4,398	P	605	P	2,039	Sdc2
1420853_at	NM_011520	Syndecan 3	A	382	A	547	P	680	P	902	A	385	P	762	Sdc3
1417654_at	NM_011521	Syndecan 4	P	306	P	281	P	244	P	342	P	305	P	320	Sdc4
1424950_at	BI077717	SRY-box containing gene 9	P	120	A	5	A	59	A	27	P	1,344	P	183	Sox9
1420895_at	BM248342	Transforming growth factor, beta receptor I	P	780	P	703	P	657	P	862	P	1,595	P	802	Tgfbr1
1425444_a_at	S69114	Transforming growth factor, beta receptor II	P	552	P	746	P	1,068	P	1,189	P	868	P	1,133	Tgfbr2
1425620_at	AF039601	Transforming growth factor, beta receptor III	P	448	A	328	A	275	P	313	P	855	P	1,015	Tgfbr3
1422912_at	NM_007554	Bone morphogenetic protein 4	P	1,048	P	646	P	6,470	P	7,266	P	1,736	P	2,890	Bmp4
1425492_at	BM248248	Bone morphogenetic protein receptor, type 1A	P	1,486	P	815	P	1,089	P	1,164	P	1,189	P	1,123	Bmpr1a
1420847_a_at	NM_010207	Fibroblast growth factor receptor 2	P	833	P	656	P	1,664	P	1,998	P	992	P	3,598	Fgfr2
1417271_a_at	NM_007932	Endoglin	A	247	A	187	A	40	A	115	A	222	P	1,371	Eng
1451314_a_at	L08431	Vascular cell adhesion molecule 1	P	462	A	39	A	28	A	92	P	812	P	583	Vcam1

The raw data from the gene chip analysis are available at our laboratory's web site (http://1954.jukuin.keio.ac.jp/umezawa/chip/sugiki). Flag indicates the presence or absence of gene expression determined by presence/absence call (Affymetrix).
P (presence): gene is expressed. M (marginal): gene is marginally expressed. A (absence): gene is not expressed.

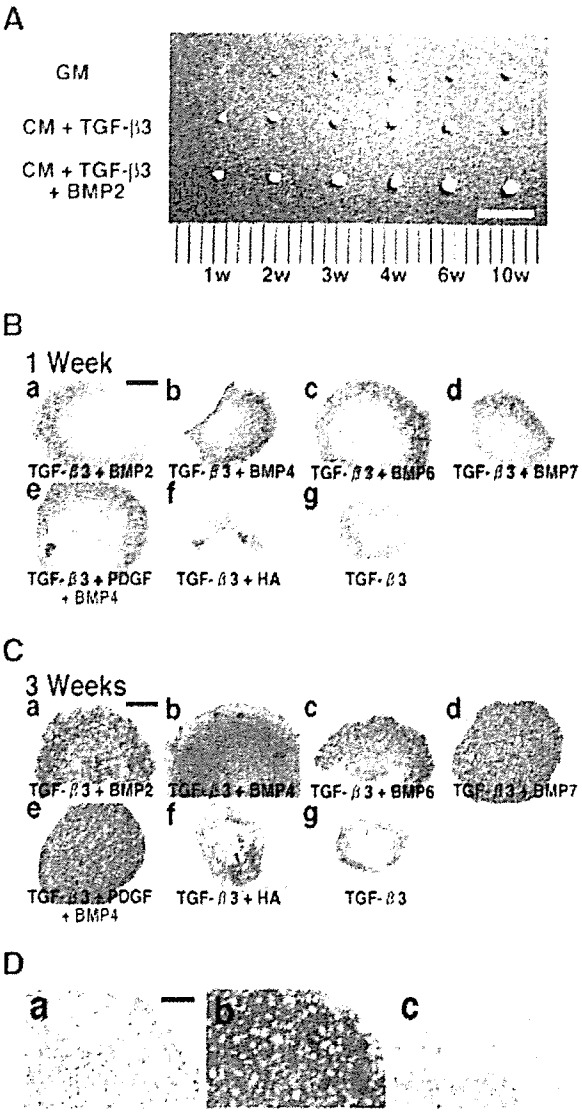

Fig. 2. In vitro chondrogenesis of OP9 cells. **A**: Time-course analysis of growth factors-induced matrix production in OP9 cells. Macroscopic view of OP9 chondrogenic nodules which were generated after pellet culture for 1–10 weeks in the GM or the CM supplemented with growth factors as indicated. BMP2 drastically enhanced TGF-β3-induced matrix production of OP9 cells. **B,C**: Microscopic view of OP9 chondrogenic nodules in the pellet culture exposed to growth factors as indicated for 1 week (B) or 3 weeks (C). **D**: OP9 chondrogenic pellet exposed to TGF-β3 and BMP2 for 3 weeks. **a**: hematoxylin and eosin stain; **b**: toluidine blue stain; **c**: alcian blue stain. Scale bars: 5 mm (A), 200 μm (B,C), 100 μm (D).

abundant extracellular matrix (Fig. 2D) and caused deeper metachromatic staining and an enlarged metachromatic area (Fig. 2Db). Additionally, we examined the effect of other cytokines on the differentiation of OP9 cells with procedures analogous to those used for KUM5 cells. BMP4, BMP6, and BMP7 enhanced the TGF-β3-induced differentiation in a manner similar to BMP2 (Fig. 2B,C). Unlike its effect in KUM5 cells, PDGF did not inhibit TGF-β3- and BMP4-induced differentiation, as determined by toluidine blue staining (Fig. 2Be,Ce). To confirm the chondrogenetic differentiation histologically, we examined the ultrastructural analysis of the cartilaginous micromasses. Extracellular matrix was abundantly deposited over OP9 cells, or the surface of the generated micromass (Fig. 3D). The cells covering the micromass showed a flattened shape (Fig. 3E). The OP9 chondrocytes inside the micromass showed an oval or round structure, had cellular processes, and were embedded in the hypertrophic chondrocytes. Abundant rough endoplasmic reticulum and a small number of mitochondria were observed in the OP9 chondrocytes (Fig. 3F).

Cell Surface Markers in KUM5 and OP9 Cells

To characterize the KUM5 and OP9 cells, we analyzed the cell surface markers by using flowcytometry. KUM5 cells were positive (more than tenfold compared to the isotype control) for CD9, CD105 (endoglin), Sca-1 and Ly-6C, marginal for CD106 (VCAM-1) and CD140a (PDGFRα), and negative for c-kit (CD117), Flk-1, CD31 (PECAM-1), CD34, CD144 (VE-cadherin), CD45 (leukocyte common antigen), CD49d (integrin α4), CD90 (Thy-1), CD102, CD14, Ly-6G, and CD41 (Fig. 4A). OP9 cells were strongly positive for CD140a, CD106, and CD9, weakly positive for Sca-1, and negative for CD105, c-kit, Flk-1, CD31, CD34, CD144, CD45, CD49d, CD90, CD102, CD14, Ly-6C, Ly-6G, and CD41 (Fig. 4B). Next, we performed hierarchical clustering by analyzing the global gene expression pattern for cell type classification and cell function prediction. When 244 cell surface marker genes are used for analysis, KUM5 and OP9 formed one cluster independent of seven other marrow stromal cells (Fig. 4C, Supplementary Table I, http://1954.jukuin.keio.ac.jp/umezawa/sugiki/pca). We then performed PCA to determine whether it is possible to discriminate OP9 and KUM5 from other cells in three-dimensional expression space. Using the same gene sets for clustering analysis, KUM5 and OP9 cells can clearly separated from the other seven cell lines (Fig. 4D). The similarity of the in vitro phenotype of KUM5 and OP9 cells was supported by the results of

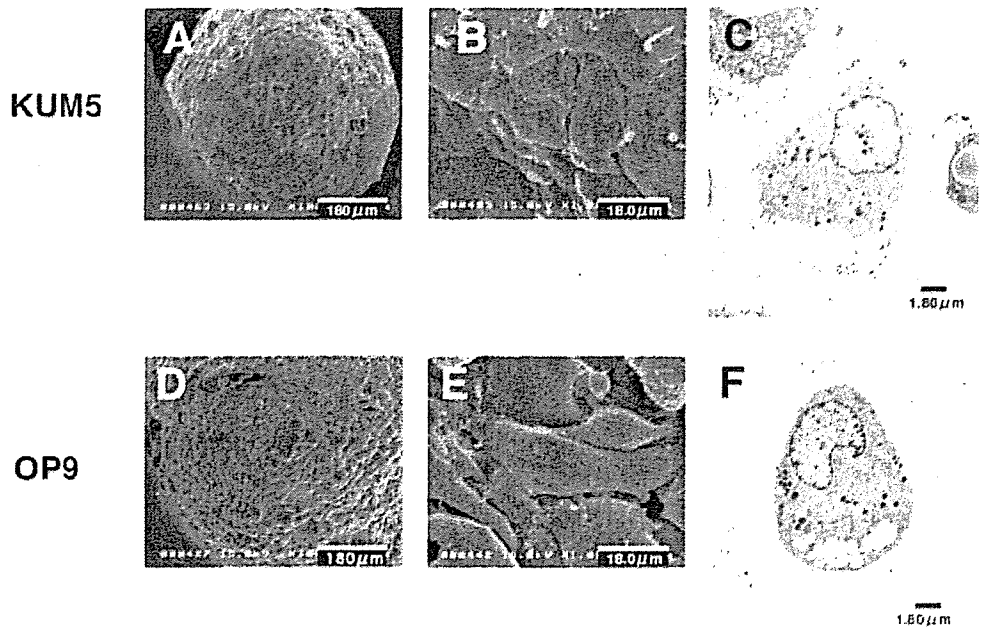

Fig. 3. Ultrastructural analysis of the in vitro chondrogenic micromass. Micromasses of KUM5 cells (**A–C**) and OP9 cells (**D–F**) were generated by culturing in the CM supplemented with TGF-β3 for 3 weeks. (A,B,D,E), SEM; (C,F), TEM.

grouping the marrow stromal cells into subcategories in terms of cell surface markers.

Global Outlook by Hierarchical Clustering and PCA by Fat- and Cartilage-Associated Genes

We also performed hierarchical clustering and PCA on the expression pattern of fat- and cartilage-associated genes. Using 34 fat-associated genes (Supplementary Table II), KUM5 and OP9 were separated and show smaller distance by both hierarchical clustering and PCA, implying that the KUM5 and OP9 cells have similar characteristics compared with other seven marrow stromal cells (Fig. 5A–D). In contrast, the analysis of 36 cartilage-associated gene expression data (Fig. 5E, Supplementary Table III) demonstrated that these two cell lines were not grouped into the same subcategory. Both cells showed "P: positive" expression in Sox9 and type II collagen α1 genes, and OP9 cells expressed cartilage-specific and -associated genes such as the type II collagen α1, type XI collagen α1, cartilage oligomeric matrix proteins, and proline arginine-rich end leucine-rich repeat genes at higher levels, when compared to KUM5 cells (Table I). These results imply that OP9 cells are differentiated chondrocytes as a default state while KUM5 cells are oligopotent mesenchymal cells that have a tendency to differentiate into chondrocytes.

In Vivo Chondrogenesis

To examine the chondrogenic activity of KUM5 cells, we injected KUM5 cells at confluence without any treatment (i.e., without TGF-β3 and BMP2 treatment) into mice subcutaneously (Fig. 6A). KUM5 cells generated cartilage-like structures within 1 week and complete cartilage at 3 weeks, and the generated cartilage exhibited metachromasia with toluidine blue staining. Interestingly, the cartilage generated by KUM5 cells showed enchondral ossification at 4 weeks. We then implanted the KUM5 chondrogenic micromass after pellet culture into the subcutaneous tissue just beneath the cutaneous muscle (Fig. 6B). The KUM5 cartilage was formed within 1 week and it exhibited typical chondrogenic structures: post-mitotic daughter cells in the cell nest, hypertrophic chondrocytes, and abundant metachromatic matrix with toluidine blue staining. The immunohistochemical analysis showed that KUM5 cartilage stained positive for chondrocyte-specific type II collagen (Fig. 6C), while only a slight amount of type II collagen was detected in the in vitro pelleted micromass culture. Ultrastructural analysis revealed that KUM5 chondrocytes implanted into the subcutaneous tissue of nude mice were embedded in the lacunae cavities and had

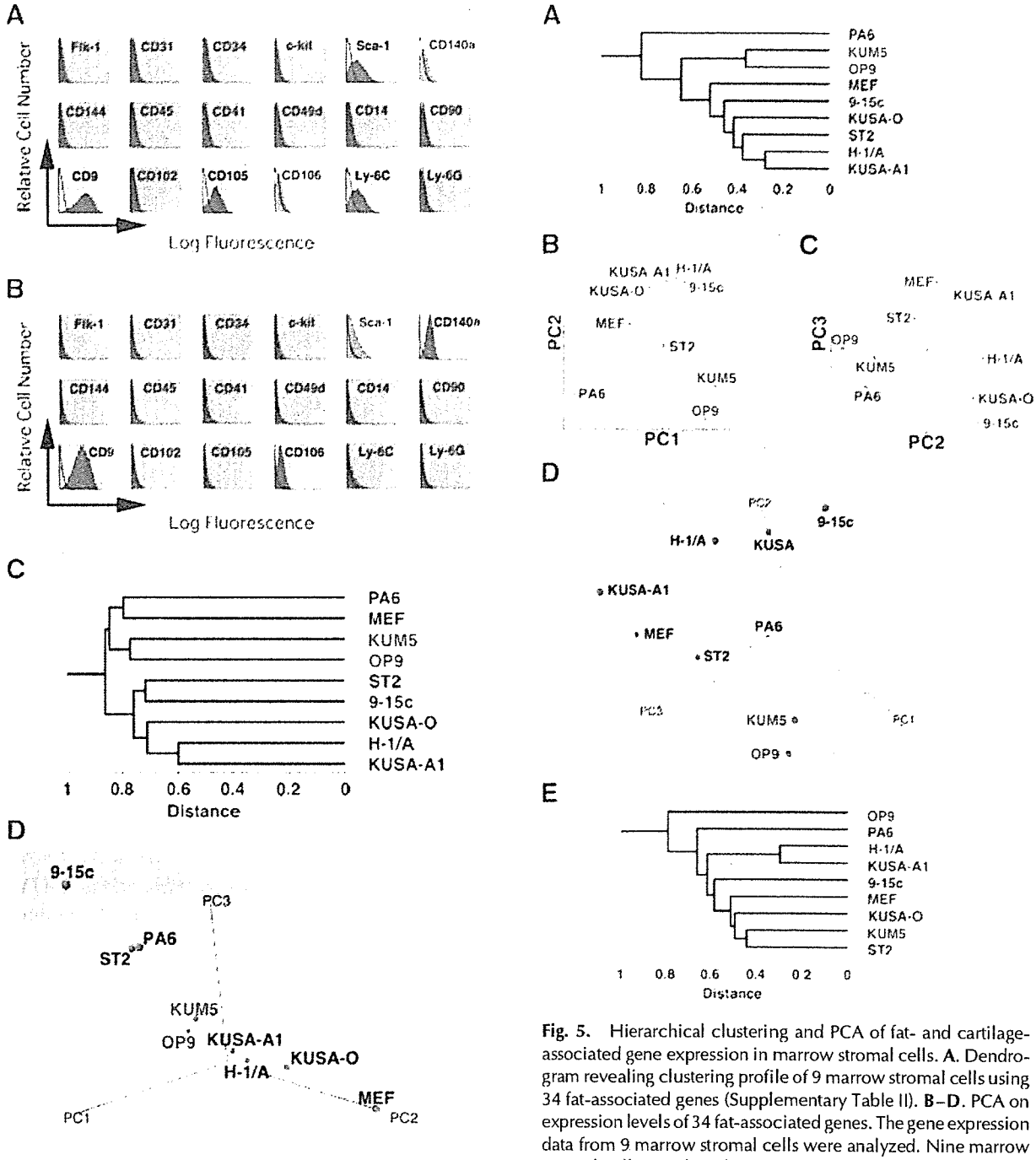

Fig. 4. Expression profiling, hierarchical clustering, and principal component analysis (PCA) of cell surface markers in marrow stromal cells. **A,B**: Flow cytometric analysis of cell surface markers in KUM5 cells (A) and OP9 cells (B). Red and pink colors indicate positive and marginal expression, respectively, and blue color indicates negative expression. **C**: Dendrogram revealing clustering profile of nine marrow stromal cells using 244 surface marker genes (Supplementary Table I). **D**: The rotated and dimensionally reduced gene expression data. Nine marrow stromal cells are plotted onto the 1st, 2nd, and 3rd principal component using 244 surface marker genes. These results indicate that KUM5 and OP9 cells were grouped into the same subcategory.

Fig. 5. Hierarchical clustering and PCA of fat- and cartilage-associated gene expression in marrow stromal cells. **A.** Dendrogram revealing clustering profile of 9 marrow stromal cells using 34 fat-associated genes (Supplementary Table II). **B–D.** PCA on expression levels of 34 fat-associated genes. The gene expression data from 9 marrow stromal cells were analyzed. Nine marrow stromal cells are plotted onto 2D-representation, PC1 and PC2 axes (B) or PC2 and PC3 axes (C), and 3D-representation (D). These results indicate that KUM5 and OP9 cells were grouped into the same subcategory. **E.** Dendrogram revealing clustering profile of 9 marrow stromal cells using 36 cartilage-associated genes (Supplementary Table III).

abundant endoplasmic reticulum and a small number of mitochondria (Fig. 6D), and collagen fibers were produced around the lacunae cavity of the KUM5 chondrocytes (Fig. 6E), as is the case of the in vitro conditions.

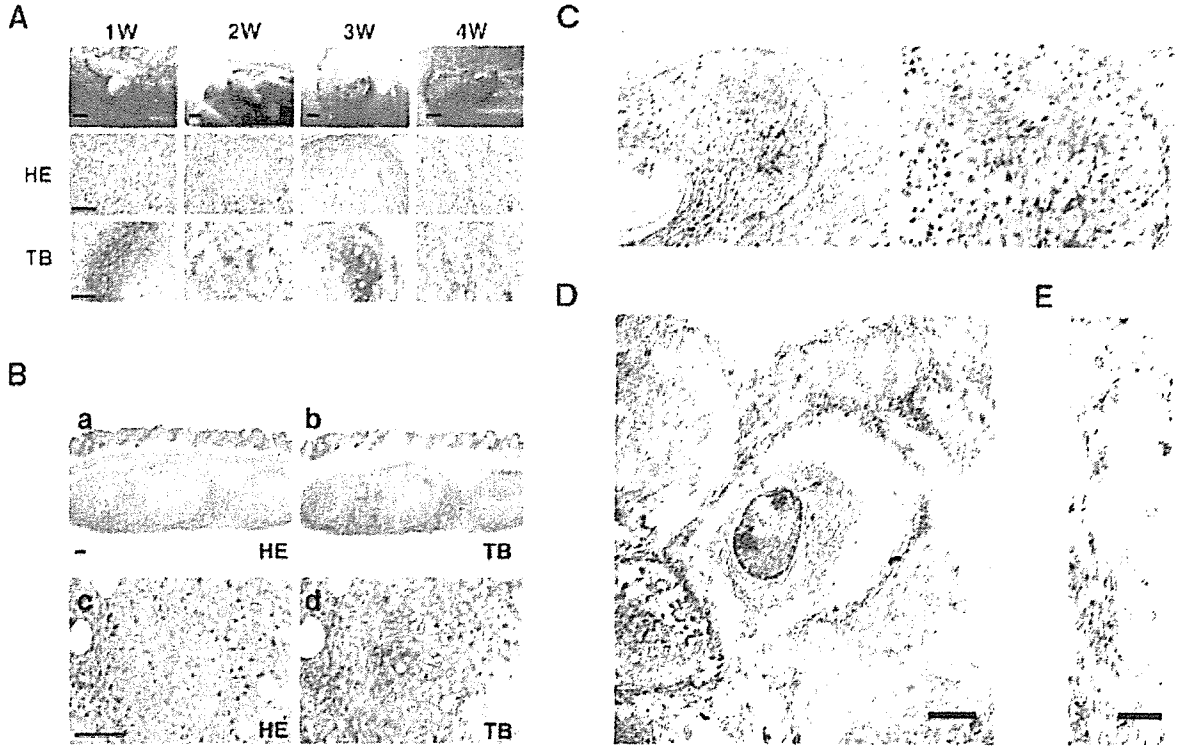

Fig. 6. In vivo chondrogenesis of KUM5 cells. **A**: Macroscopic view (**top**), hematoxylin and eosin stain (HE) (**middle**) and toluidine blue stain (TB) (**bottom**) analysis at 1, 2, 3, and 4 week (w)-cultivation in vivo after direct injection of KUM5 cells. **B**: KUM5 chondrogenic nodules, that were generated after pellet culture for 7 days in the CM supplemented with TGF-β3 and BMP2, were implanted just beneath the cutaneous muscle in the subcutaneous tissue and were cultivated in vivo for 3 weeks. **Panels c** and **d** are higher magnifications of **a** and **b**, respectively. **C**: Expression of chondrocyte-specific type II collagen. The KUM5 chondrogenic nodules were sectioned after 2 week-in vivo cultivation and stained with collagen type II-specific antibody. **D,E**: Ultrastructural analysis (TEM) of KUM5 implants. KUM5 cells were implanted into the subcutaneous tissue of Balb/c nu/nu mice, and the generated cartilage was resected 2 weeks after implantation. Scale bars: 2 mm (A, top row), 100 μm (A, middle and bottom row), 100 μm (B), 2 μm (D), 1 μm (E).

To determine the chondrogenic activity of OP9 cells in vivo, we directly injected them into the subcutaneous tissue. The OP9 cells without any induction did not generate cartilage. We then implanted the OP9 chondrogenic micromass after the pellet culture into the subcutaneous tissue just beneath the cutaneous muscle (Fig. 7A,B). The OP9 cartilage was formed at 2 and 4 weeks, and abundant metachromatic matrix was observed with the toluidine blue stain. The immunohistochemical analysis shows that OP9 cartilage stains positive for the chondrocyte-specific type II collagen (Fig. 7C).

Sorting of Chondroblasts by Chondrocyte-Specific Cis-Regulatory Element of the Collagen α2(XI) Gene

Although the KUM5 cells used in this study were derived from a single-cell origin or clone, it could be argued that both cells responsive and non-responsive to chondrogenic induction were present [Ko et al., 1990]. In this sense, KUM5 cells might have been a largely heterogeneous cell population. Even cells derived from a single clone have been shown to be heterogeneous in terms of differentiation capacity and stages [Muraglia et al., 2000]. To validate the chondrogenic differentiation observed here, a homogenous population of committed cell obtained after induction should be isolated. Therefore, for the purpose of sorting chondrogenically committed cells, we transfected KUM5 cells with a Venus-expression vector under the control of the Col α2(XI) promoter, analyzed the transfected cells, and collected Venus-positive cells (Fig. 8A–D). The sorted cells were assessed for in vitro (Fig. 9A–F) and in vivo chondrogenesis (Fig. 9G–I). The cells again showed metachromatic chondrogenic micromasses with toluidine blue staining in vitro (Fig. 9B). Direct injection of the cells resulted in the cartilage formation within 1 week and obvious enchondral ossification at the periphery

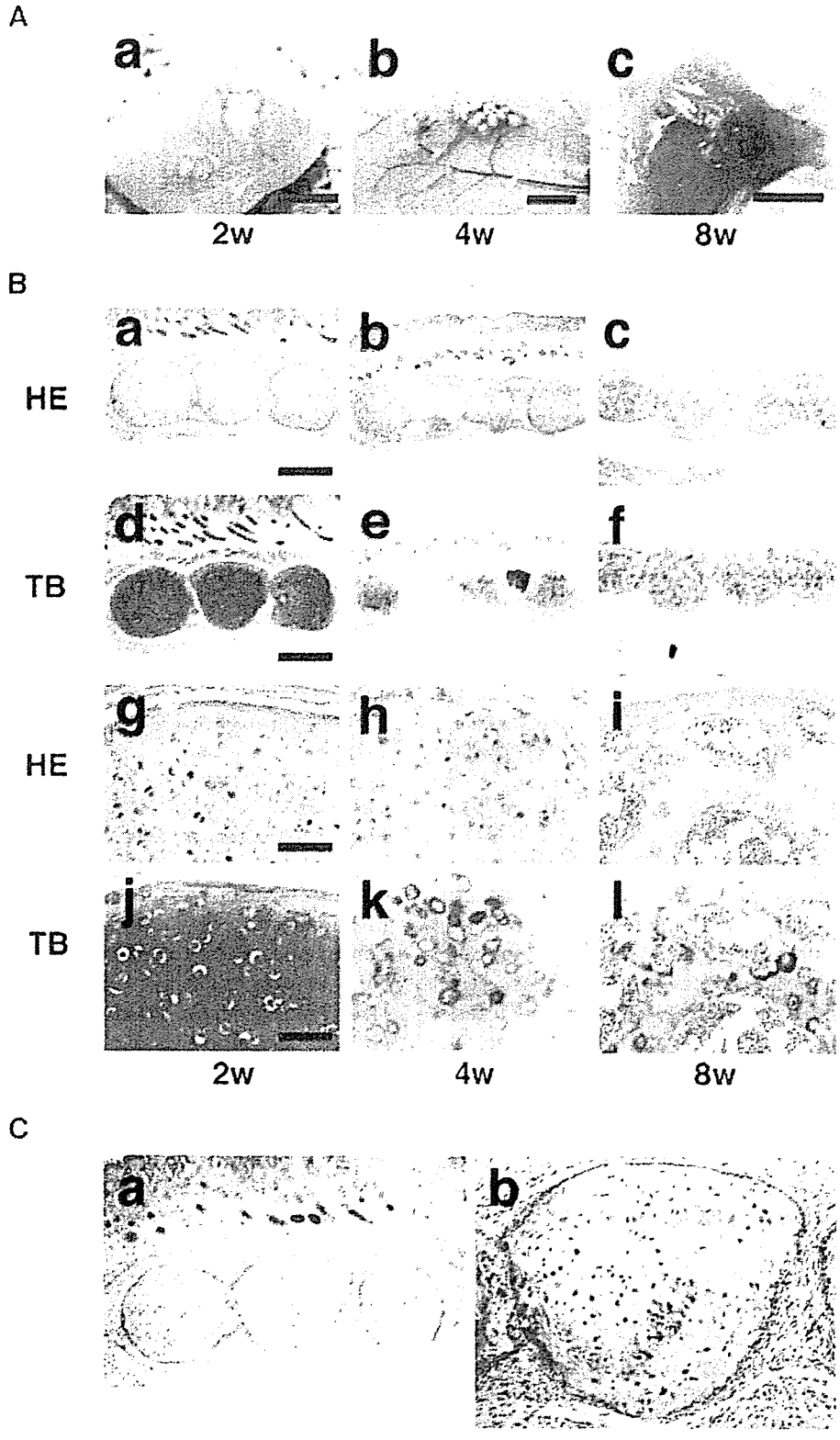

Fig. 7. In vivo chondrogenesis of OP9 cells. In vivo chondrogenesis was examined by implantation of OP9 chondrogenic nodules. OP9 chondrogenic nodules, which were generated after pellet culture for 7 days in the CM supplemented with TGF-β3 and BMP2, were implanted just beneath the cutaneous muscle in the subcutaneous tissue and were cultivated in vivo for the number of weeks indicated. **A**: Macroscopic view of OP9 cartilage after 2 (a), 4 (b), and 8 (c)-week-in vivo cultivation. **B**: Histological analysis of OP9 cartilage after 2 (**a**,**d**,**g**,**j**), 4 (**b**,**e**,**h**,**k**), and 8 (**c**,**f**,**i**,**l**)-week-in vivo cultivation. (a,b,c,g,h,i), HE stain; (d,e,f,j,k,l), TB stain. **Panels g–l** are higher magnifications of **a–f**, respectively. **C**: Immunohistochemical analysis of the in vivo OP9 chondrogenic nodules. The OP9 chondrogenic nodules after 2-week-in vivo cultivation stained positive for type II collagen. Scale bars: 2 mm (A), 500 μm (Ba–f), 100 μm (Bg–l).

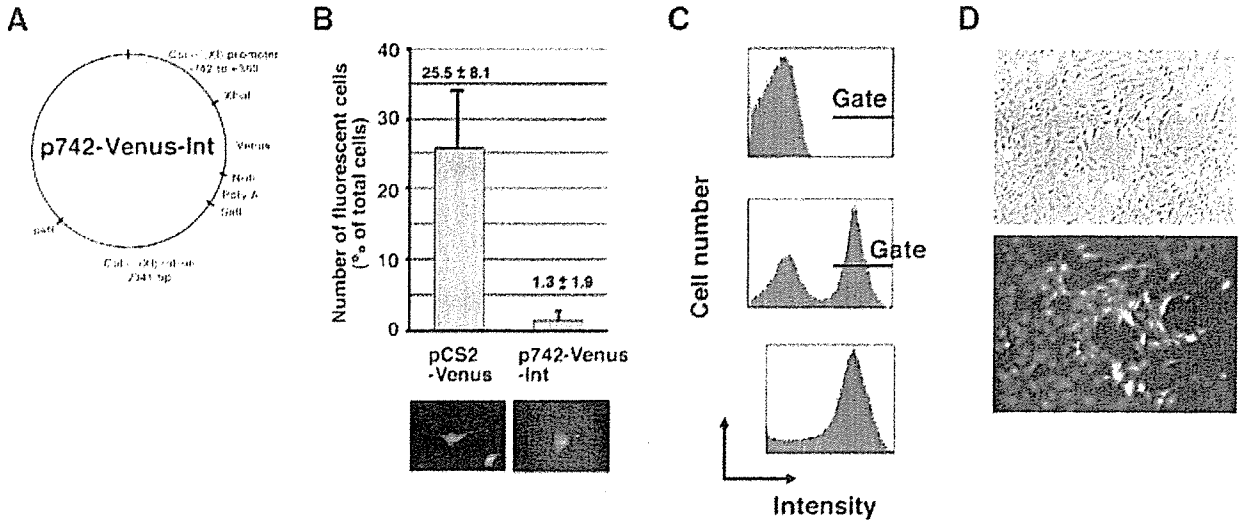

Fig. 8. Isolation of KUM5 chondroblasts using the chondroblast-specific cis-regulatory element. **A**: The p742-Venus-Int plasmid containing the fluorescent Venus gene driven by the cis-regulatory elements of the α2(XI) collagen gene. **B**: The number of fluorescent KUM5 cells (**upper**) after transfection with the p742-Venus-Int plasmid or pCS2-Venus containing the Venus gene driven by the CMV-promoter. Fluorescent photomicrograph of KUM5 cells after the first sorting (**lower**). **C**: Flowcytometric analysis of KUM5 cells after transfection with the p742-Venus-Int plasmid (**top**); The fluorescence-positive cells were sorted, propagated, and analyzed (**middle**). Again, the propagated fluorescence-positive cells were sorted, propagated, and analyzed (**bottom**). The "gate" for sorting is shown by the horizontal bar in the upper and middle panels. More than 80% of cells became positive after the final sorting. **D**: Phase contrast micrograph (upper) and fluorescent photomicrograph (lower) of the finally sorted cells (the lower panel of C).

of the cartilage at 4 weeks (Fig. 9G). Again, ultrastructural analysis revealed that KUM5 chondrocytes implanted into the subcutaneous tissue of nude mice were embedded in the hypertrophic chondrocytes and had abundant endoplasmic reticulum and a small number of mitochondria (Fig. 9H,I). The post-mitotic daughter cells in the cell nest, which are often observed in cartilage, were also detected (Fig. 9I).

DISCUSSION

In this study, we focus on the chondrogenic differentiation in vitro and in vivo using the two cell lines, KUM5 and OP9. The chondrogenic process is determined by the sequential expression of matrix component, and the differential response of differentiating cells to the growth factors may be attributed to the differentiating stages that depend on the expression patterns of the gene set as is the case for hematopoietic cells. The process of the chondrogenic differentiation is influenced by a number of growth factors including TGF-β and/or BMPs. Three isoforms of TGF-β have been known to have the ability to induce the chondrogenic differentiation. Both TGF-β2 and -β3 are more effective than TGF-β1 in promoting chondrogenesis, and TGF-β3 accelerates production of cartilaginous extracellular matrix in differentiating mesenchymal stem cells [Barry et al., 2001].

This study was undertaken to obtain mesenchymal stem cells with chondrogenic potential that retain critical in vivo cell functions, as do mammary gland epithelial cells, skin keratinocytes, and pigmented epithelial cells. To achieve this, we attempted to identify marrow-derived cells with chondrogenic nature and immortality without transformation among the cells obtained by the limiting-dilution method [Umezawa et al., 1992], defining "immortality" simply as indefinite cell division.

OP9 cells are known to serve as a niche or a specific microenvironment for the regulation of self-renewal and differentiation of stem cells [Nakano, 1996], and the question is raised of whether marrow stromal cells or marrow-derived mesenchymal cells with chondrogenic potential are capable of constituting a microenvironment for stem cells. It is inconceivable that cartilage can form a niche for cells in the living body based on structural and morphological considerations; however, a cell with chondrogenic or adipo-chondrogenic potential may serve as a niche not only in the case of OP9 cells but also as a general concept, at least in vitro.

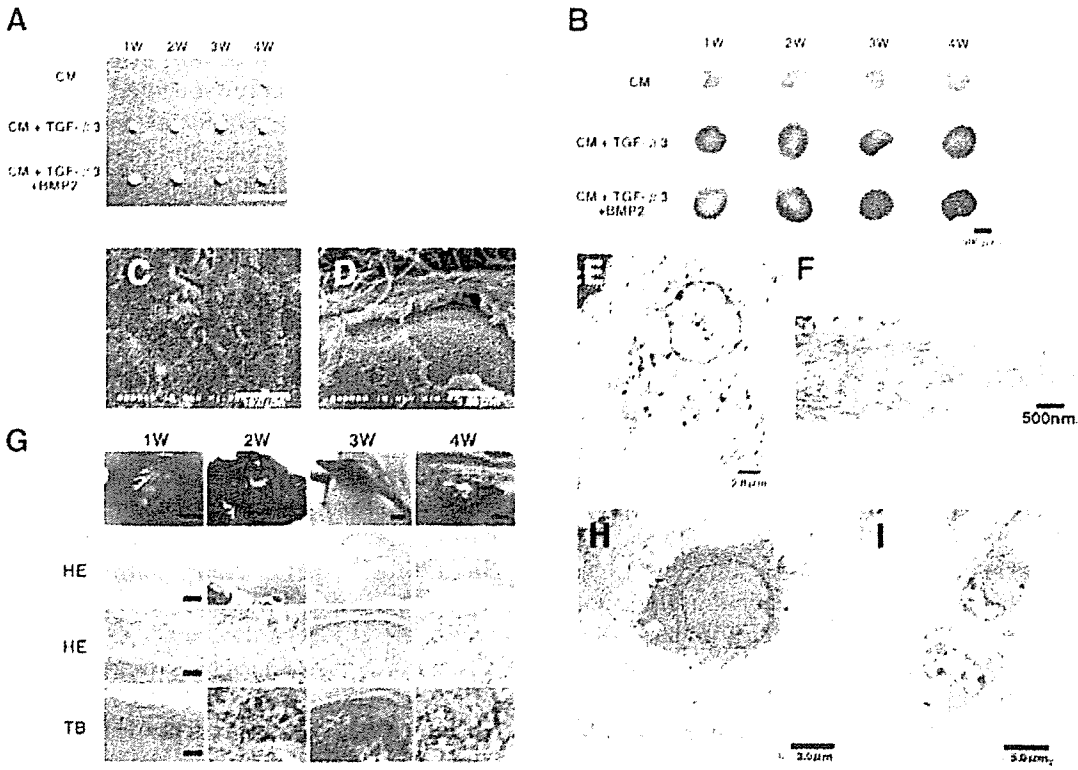

Fig. 9. In vitro and in vivo chondrogenesis of KUM5 cells sorted according to the activity of the chondrocyte-specific cis-regulatory element. **A,B**: Macroscopic view of the chondrogenic nodules which were generated after pellet culture of the finally sorted KUM5 cells for 1–4 weeks in the CM supplemented with growth factors as indicated (A) and toluidine blue stained section (B). **C–F**: Ultrastructural analysis of the micromasses of KUM5 cells sorted according to the activity of the Col α2(XI) cis-regulatory element (KUM5-Venus) after culturing in the CM supplemented with TGF-β3 for 3 weeks. (C,D), SEM; (E,F), TEM. **G**: In vivo chondrogenesis was examined 1–4 weeks after direct injection of the finally sorted KUM5 cells. From top to bottom: Macroscopic view, histological analysis, HE stain; histological analysis, HE stain; histological analysis, TB stain. **H,I**: Ultrastructural analysis (TEM) of the sorted KUM5 cartilage. The sorted KUM5 cells were implanted into the subcutaneous tissue of Balb/c nu/nu mice, and the generated cartilage was resected 2 weeks after implantation. Scale bars: 5 mm (A), 500 μm (B), 2 mm (G, **top row**), 500 μm (G, **2nd row**), 100 μm (G, **3rd** and **bottom row**).

The sequence of enchondral or perichondral ossification by KUM5 and OP9 cells was as follows: deposition of homogeneous matrix surrounding the small nests of the injected cells that subsequently became positive for type II collagen and exhibited metachromasia with toluidine blue staining, trapping them in the secreted homogeneous matrix, and the appearance of small nests of isogenous chondrocytes that probably resulted from repeated cell division. At a later stage, that is, 4–8 weeks after injection, the peripheral region of the generated cartilage became ossified. Importantly, the chondrogenesis by KUM5 and OP9 cells was irreversible and reproducible, and the implanted cells never transformed into malignant cells, formed any abnormal extracellular matrices, or induced any significant inflammatory reactions. It is again noteworthy that the osteogenesis by these two different lines of cells was mediated by chondrogenesis, and it was therefore considered to be chondral ossification. Thus, the unique characteristics of these two cell lines provide an opportunity to analyze the process of enchondral or perichondral ossification in an experimental system in detail.

In fetal life, primary ossification centers form by one of two processes: enchondral ossification or membranous ossification. Enchondral ossification refers to bony replacement of cartilage and is the mode of formation of the long bones. During membranous ossification mesenchymal cells form membranes within which ossification occurs and this is the mode of formation of the scapula and skull and, in part, of the clavicle and pelvis. After birth, bone growth continues by both enchondral and membranous ossification. Further enchondral ossification occurs in

the physes and results in continuous longitudinal growth of the long bones until skeletal maturity. KUM5 and OP9 cells were obtained from long bone and calvaria, respectively, and showed enchondral ossification. We have also reported that KUSA-A1 cells form bone by membranous ossification in vivo, and thus we have three different types of cells showing distinctive in vivo characteristics. The process of chondrogenesis or enchondral ossification may also serve as a model for chondromatosis and osteochondromatosis in a joint cavity.

The expression pattern of chondrocyte-specific genes in OP9 and KUM5 cells is different from that in ATDC5 cells, which are a mouse embryonal carcinoma-derived chondrogenic cell line. ATDC5 cells exhibit a multistep differentiation process encompassing the stages from chondrogenesis to enchondral ossification [Shukunami et al., 1996]. Early-phase differentiation is characterized by the expression of type II collagen, followed by induction of the aggrecan gene. Late stage differentiation is characterized by the start of expression of short-chain collagen type X genes. By contrast, marrow-derived mesenchymal stem cells express the aggrecan genes at an early stage and then type II collagen during chondrogenic differentiation [Pittenger et al., 1999]. Surprisingly, gene expression pattern determined by the gene chip analysis was consistent with protein levels of cell surface molecules; this consistency indicates that the expression profiling is valid. Expression of "structural proteins" on Gene Ontology, including the extracellular matrix, was much higher by OP9 and KUM5 cells than by non-chondrogenic cells such as KUSA-A1 osteoblasts, H-1/A preadipocytes, and 9-15c mesenchymal stem cells, implying that the OP9 and KUM5 cells are mainly engaged in synthesizing extracellular matrix.

Can we inhibit enchondral or perichondral ossification after the completion of chondrogenesis? This is a challenge for the future, probably the not-too-distant future. We could not prevent the generated hyaline cartilage from ossifying at present even after selection based on the chondrocyte-specific cis-regulatory element of the collagen α2(XI) gene, probably due to the inability to inhibit vasculogenesis from the neighboring connective tissue. However, these established murine marrow-derived mesenchymal cells with in vivo chondrogenic activity and expression profiles provide a powerful model for studies of chondrogenic differentiation and our further understanding of cartilage regeneration. Bone marrow-derived chondroblasts with chondrogenic potential are useful candidate cell sources in addition to dedifferentiated chondrocytes obtained from cartilage for transplantation in osteoarthritis and rheumatoid arthritis.

ACKNOWLEDGMENTS

We would like to express our sincere thanks to Shin-ichiro Takayama, Yasushi Nakao, Hiroyasu Ikegami, and Toshiyasu Nakamura for support throughout the work, Atsushi Miyawaki for the Venus/pCS2 plasmid, Kayoko Saito for secretarial assistance, and Toshihiro Nagai and Yoshie Hashimoto for providing expert technical assistance. This study was supported by grants from the Ministry of Education, Culture, Sports, Science, and Technology (MEXT) of Japan, the Health; Labour Sciences Research Grants, and the Pharmaceuticals and Medical Devices Agency; by Research on Health Science focusing on Drug Innovation (KH71064) from the Japan Health Science Foundation; by the program for promotion of fundamental Studies in Health Science of the Pharmaceuticals and Medical Devices Agency (PMDA); by the research Grant for Cardiovascular Disease (H16C-6) from the ministry of Health, Labour and Welfare; by supported by a Grant for Child Health and Development (H15C-2) from the Ministry of Health, Labour and Welfare. The raw data from the gene chip analysis is available at our laboratory's web site (http://1954.jukuin.keio.ac.jp/umezawa/chip/sugiki/index.html). The photomicrographs of the pelleted micromasses examined by SEM and TEM were available at http://1954.jukuin.keio.ac.jp/umezawa/sugiki/EM/index.html. The wrl files of the 3D-representation of PCA are available at http://1954.jukuin.keio.ac.jp/umezawa/sugiki/pca/index.html.

REFERENCES

Archer CW, McDowell J, Bayliss MT, Stephens MD, Bentley G. 1990. Phenotypic modulation in sub-populations of human articular chondrocytes in vitro. J Cell Sci 97(Pt 2):361–371.

Barry F, Boynton RE, Liu B, Murphy JM. 2001. Chondrogenic differentiation of mesenchymal stem cells from bone marrow: Differentiation-dependent gene expression of matrix components. Exp Cell Res 268:189–200.

Benya PD, Shaffer JD. 1982. Dedifferentiated chondrocytes reexpress the differentiated collagen phenotype when cultured in agarose gels. Cell 30:215–224.

Bianco P, Robey PG. 2000. Marrow stromal stem cells. J Clin Invest 105:1663–1668.

Bonaventure J, Kadhom N, Cohen-Solal L, Ng KH, Bourguignon J, Lasselin C, Freisinger P. 1994. Reexpression of cartilage-specific genes by dedifferentiated human articular chondrocytes cultured in alginate beads. Exp Cell Res 212:97–104.

Fujii M, Takeda K, Imamura T, Aoki H, Sampath TK, Enomoto S, Kawabata M, Kato M, Ichijo H, Miyazono K. 1999. Roles of bone morphogenetic protein type I receptors and Smad proteins in osteoblast and chondroblast differentiation. Mol Biol Cell 10:3801–3813.

Hauselmann HJ, Fernandes RJ, Mok SS, Schmid TM, Block JA, Aydelotte MB, Kuettner KE, Thonar EJ. 1994. Phenotypic stability of bovine articular chondrocytes after long-term culture in alginate beads. J Cell Sci 107: 17–27.

Johnstone B, Hering TM, Caplan AI, Goldberg VM, Yoo JU. 1998. In vitro chondrogenesis of bone marrow-derived mesenchymal progenitor cells. Exp Cell Res 238:265–272.

Ko MS, Nakauchi H, Takahashi N. 1990. The dose dependence of glucocorticoid-inducible gene expression results from changes in the number of transcriptionally active templates. EMBO J 9:2835–2842.

Kohyama J, Abe H, Shimazaki T, Koizumi A, Nakashima K, Gojo S, Taga T, Okano H, Hata J, Umezawa A. 2001. Brain from bone: Efficient "meta-differentiation" of marrow stroma-derived mature osteoblasts to neurons with Noggin or a demethylating agent. Differentiation 68:235–244.

Lefebvre V, Peeters-Joris C, Vaes G. 1990. Production of collagens, collagenase and collagenase inhibitor during the dedifferentiation of articular chondrocytes by serial subcultures. Biochim Biophys Acta 1051:266–275.

Maeda S, Hayashi M, Komiya S, Imamura T, Miyazono K. 2004. Endogenous TGF-beta signaling suppresses maturation of osteoblastic mesenchymal cells. EMBO J 23:552–563.

Makino S, Fukuda K, Miyoshi S, Konishi F, Kodama H, Pan J, Sano M, Takahashi T, Hori S, Abe H, Hata J, Umezawa A, Ogawa S. 1999. Cardiomyocytes can be generated from marrow stromal cells in vitro. J Clin Invest 103:697–705.

Mori T, Kiyono T, Imabayashi H, Takeda Y, Tsuchiya K, Miyoshi S, Makino H, Matsumoto K, Saito H, Ogawa S, Sakamoto M, Hata J, Umezawa A. 2005. Combination of hTERT and bmi-1, E6, or E7 induces prolongation of the life span of bone marrow stromal cells from an elderly donor without affecting their neurogenic potential. Mol Cell Biol 25:5183–5195.

Muraglia A, Cancedda R, Quarto R. 2000. Clonal mesenchymal progenitors from human bone marrow differentiate in vitro according to a hierarchical model. J Cell Sci 113(Pt 7):1161–1166.

Nagai T, Ibata K, Park ES, Kubota M, Mikoshiba K, Miyawaki A. 2002. A variant of yellow fluorescent protein with fast and efficient maturation for cell-biological applications. Nat Biotechnol 20:87–90.

Nakano T. 1996. In vitro development of hematopoietic system from mouse embryonic stem cells: A new approach for embryonic hematopoiesis. Int J Hematol 65:1–8.

Nakano T, Kodama H, Honjo T. 1994. Generation of lymphohematopoietic cells from embryonic stem cells in culture. Science 265:1098–1101.

Ochi K, Chen G, Ushida T, Gojo S, Segawa K, Tai H, Ueno K, Ohkawa H, Mori T, Yamaguchi A, Toyama Y, Hata J, Umezawa A. 2003. Use of isolated mature osteoblasts in abundance acts as desired-shaped bone regeneration in combination with a modified poly-DL-lactic-co-glycolic acid (PLGA)-collagen sponge. J Cell Physiol 194: 45–53.

Pittenger MF, Mackay AM, Beck SC, Jaiswal RK, Douglas R, Mosca JD, Moorman MA, Simonetti DW, Craig S, Marshak DR. 1999. Multilineage potential of adult human mesenchymal stem cells. Science 284:143–147.

Reginato AM, Iozzo RV, Jimenez SA. 1994. Formation of nodular structures resembling mature articular cartilage in long-term primary cultures of human fetal epiphyseal chondrocytes on a hydrogel substrate. Arthritis Rheum 37:1338–1349.

Shukunami C, Shigeno C, Atsumi T, Ishizeki K, Suzuki F, Hiraki Y. 1996. Chondrogenic differentiation of clonal mouse embryonic cell line ATDC5 in vitro: Differentiation-dependent gene expression of parathyroid hormone (PTH)/PTH-related peptide receptor. J Cell Biol 133: 457–468.

Terai M, Uyama T, Sugiki T, Li XK, Umezawa A, Kiyono T. 2005. Immortalization of human fetal cells: The life span of umbilical cord blood-derived cells can be prolonged without manipulating p16INK4a/RB breaking pathway. Mol Biol Cell 16:1491–1499.

Tsumaki N, Kimura T, Matsui Y, Nakata K, Ochi T. 1996. Separable cis-regulatory elements that contribute to tissue- and site-specific alpha 2(XI) collagen gene expression in the embryonic mouse cartilage. J Cell Biol 134:1573–1582.

Umezawa A, Tachibana K, Harigaya K, Kusakari S, Kato S, Watanabe Y, Takano T. 1991. Colony-stimulating factor 1 expression is down-regulated during the adipocyte differentiation of H-1/A marrow stromal cells and induced by cachectin/tumor necrosis factor. Mol Cell Biol 11:920–927.

Umezawa A, Maruyama T, Segawa K, Shadduck RK, Waheed A, Hata J. 1992. Multipotent marrow stromal cell line is able to induce hematopoiesis in vivo. J Cell Physiol 151:197–205.

balt2/zmk-mbc/zmk-mbc/zmk00507/zmk8034-07z | xppws | S=1 | 2/26/07 | 6:51 | 4/Color Figure(s): F1–6 | Art: 3198875 | Input-cip

Molecular Biology of the Cell
Vol. 18, 000–000, May 2007

Menstrual Blood-derived Cells Confer Human Dystrophin Expression in the Murine Model of Duchenne Muscular Dystrophy via Cell Fusion and Myogenic Transdifferentiation[D]

ChangHao Cui,*† Taro Uyama,* Kenji Miyado,* Masanori Terai,* Satoru Kyo,‡ Tohru Kiyono,§ and Akihiro Umezawa*

*Department of Reproductive Biology and Pathology, National Institute for Child Health and Development, Tokyo, 157-8567, Japan; †Department of Basic Medical Science, Mudanjiang Medical College, Mudanjiang, 157011, China; ‡Department of Obstetrics and Gynecology, Kanazawa University, School of Medicine, Kanazawa, 920-8640, Japan; and §Virology Division, National Cancer Center Research Institute, Tokyo, 104-0045, Japan

Submitted September 28, 2006; Revised January 19, 2007; Accepted February 6, 2007
Monitoring Editor: M. Bishr Omary

Duchenne muscular dystrophy (DMD), the most common lethal genetic disorder in children, is an X-linked recessive muscle disease characterized by the absence of dystrophin at the sarcolemma of muscle fibers. We examined a putative endometrial progenitor obtained from endometrial tissue samples to determine whether these cells repair muscular degeneration in a murine mdx model of DMD. Implanted cells conferred human dystrophin in degenerated muscle of immunodeficient mdx mice. We then examined menstrual blood–derived cells to determine whether primarily cultured nontransformed cells also repair dystrophied muscle. In vivo transfer of menstrual blood–derived cells into dystrophic muscles of immunodeficient mdx mice restored sarcolemmal expression of dystrophin. Labeling of implanted cells with EGFP and differential staining of human and murine nuclei suggest that human dystrophin expression is due to cell fusion between host myocytes and implanted cells. In vitro analysis revealed that endometrial progenitor cells and menstrual blood–derived cells can efficiently transdifferentiate into myoblasts/myocytes, fuse to C2C12 murine myoblasts by in vitro coculturing, and start to express dystrophin after fusion. These results demonstrate that the endometrial progenitor cells and menstrual blood–derived cells can transfer dystrophin into dystrophied myocytes at a high frequency through cell fusion and transdifferentiation in vitro and in vivo.

AQ:1

INTRODUCTION

Skeletal muscle consists predominantly of syncytial fibers with peripheral, postmitotic myonuclei, and its intrinsic repair potential in adulthood relies on the persistence of a resident reserve population of undifferentiated mononuclear cells, termed "satellite cells." In mature skeletal muscle, most satellite cells are quiescent and are activated in response to environmental cues, such as injury, to mediate postnatal muscle regeneration. After division, satellite cell progeny, termed myoblasts, undergo terminal differentiation and become incorporated into muscle fibers (Bischoff, 1994). Myogenesis is regulated by a family of myogenic transcription factors including MyoD, Myf5, myogenin, and MRF4 (Sabourin and Rudnicki, 2000). During embryonic development, MyoD and Myf5 are involved in the establishment of the skeletal muscle lineage (Rudnicki *et al.*, 1993), whereas myogenin is required for terminal differentiation (Hasty *et al.*, 1993; Nabeshima *et al.*, 1993). During muscle repair, satellite cells recapitulate the expression program of the myogenic genes manifested during embryonic development.

Dystrophin is associated with a large oligomeric complex of glycoproteins that provide linkage to the extracellular membrane (Ervasti and Campbell, 1991). In Duchenne muscular dystrophy (DMD), the absence of dystrophin results in destabilization of the extracellular membrane-sarcolemma-cytoskeleton architecture, making muscle fibers susceptible to contraction-associated mechanical stress and degeneration. In the first phase of the disease, new muscle fibers are formed by satellite cells. After depletion of the satellite cell pool in childhood, skeletal muscles degenerate progressively and irreversibly and are replaced by fibrotic tissue (Cossu and Mavilio, 2000). Like DMD patients, the mdx mouse lacks dystrophin in skeletal muscle fibers (Hoffman *et al.*, 1987; Sicinski *et al.*, 1989). However, the mdx mouse develops only a mild dystrophic phenotype, probably because muscle regeneration by satellite cells is efficient for most of the animal's life span (Cossu and Mavilio, 2000).

Myoblasts represent the natural first choice in cellular therapeutics for skeletal muscle because of their intrinsic myogenic commitment (Grounds *et al.*, 2002). However, myoblasts recovered from muscular biopsies are poorly expandable in vitro and rapidly undergo senescence (Cossu and Mavilio, 2000). An alternative source of muscle progenitor cells is therefore desirable. Cells with a myogenic potential are present in many tissues, and these cells readily

This article was published online ahead of print in *MBC in Press* (http://www.molbiolcell.org/cgi/doi/10.1091/mbc.E06–09–0872) on February 21, 2007.

[D] The online version of this article contains supplemental material at *MBC Online* (http://www.molbiolcell.org).

Address correspondence to: Akihiro Umezawa (umezawa@1985.jukuin.keio.ac.jp).

<zjs;Article> • <zjss;Articles> • <zdoi;10.1091/mbc.E06-09-0872>

form skeletal muscle in culture (Gerhart *et al.*, 2001). We report here that human dystrophin expression in the mdx model of DMD is attributed to cell fusion of mdx myocytes with human menstrual blood–derived stromal cells.

MATERIALS AND METHODS

Isolation of Human Endometrial Cells from Menstrual Blood

Menstrual blood samples (n = 21) were collected in DMEM with antibiotics (final concentrations: 100 U/ml penicillin/streptomycin) and 2% fetal bovine serum (FBS), and processed within 24 h. Ethical approval for tissue collection was granted by the Institutional Review Board of the National Research Institute for Child Health and Development, Japan. The centrifuged pellets containing endometrium-derived cells were resuspended in high-glucose DMEM medium (10% FBS, penicillin/streptomycin), maintained at 37°C in a humidified atmosphere containing 5% CO_2, and allowed to attach for 48 h. Nonadherent cells were removed by changing the medium. When the culture reached subconfluence, the cells were harvested with 0.25% trypsin and 1 mM EDTA and plated to new dishes. After 2–3 passages, the attached endometrial stromal cells were devoid of blood cells. Human EM-E6/E7/hTERT-2 cells, endometrium-derived progenitors, were obtained from surgical endometrial tissue samples and were immortalized by E6, E7, and hTERT-2 (Kyo *et al.*, 2003). C2C12 myoblast cells were supplied by RIKEN Cell Bank (The Institute of Physical and Chemical Research, Japan).

Flow Cytometric Analysis

Flow cytometric analysis was performed as previously described (Terai *et al.*, 2005). Cells were incubated with primary antibodies or isotype-matched control antibodies, followed by additional treatment with the immunofluorescent secondary antibodies. Cells were analyzed on an EPICS ALTRA analyzer (Beckman Coulter, Fullerton, CA). Antibodies against human CD13, CD14, CD29, CD31, CD34, CD44, CD45, CD50, CD54, CD55, CD59, CD73, CD90, CD105, CD117 (c-kit), CD133, HLA-ABC, and HLA-DR were purchased from Beckman Coulter, Immunotech (Marseille, France), Cytotech (Hellebaek, Denmark), and BD Biosciences PharMingen (San Diego, CA).

In Vitro Lentivirus-mediated Gene (EGFP) Transfer into EM-E6/E7/hTERT-2 Cells

Infection of EM-E6/E7/hTERT-2 cells with lentivirus having a CMV promoter and EGFP reporter resulted in high levels of EGFP expression in all cells. Cells were analyzed for EGFP expression by flow cytometry (Miyoshi *et al.*, 1997, 1998).

In Vitro Myogenesis

Menstrual blood–derived cells or EM-E6/E7/hTERT-2 cells were seeded onto collagen I–coated cell culture dishes (Biocoat, BD Biosciences, Bedford, MA) at a density of 1×10^4/ml in growth medium (DMEM, supplemented with 20% FBS). Forty-eight hours after seeding onto collagen I–coated dishes, cells were treated with 5-azacytidine for 24 h. Cell cultures were then washed twice with PBS and maintained in differentiation medium (DMEM, supplemented with either 2% horse serum (HS) or 1% insulin-transferrin-selenium supplement [ITS]). The differentiation medium was changed twice a week until the experiment was terminated.

RT-PCR Analysis of EM-E6/E7/hTERT-2 Cells and Menstrual Blood–derived Cells

Total RNA was prepared using Isogen (Nippon Gene, Tokyo, Japan). Human skeletal muscle RNA was purchased from TOYOBO (Osaka, Japan). RT-PCR of Myf5, MyoD, desmin, myogenin, myosin heavy chain-IIx/d (MyHC-IIx/d), and dystrophin was performed with 2 μg of total RNA. RNA for RT-PCR was converted to cDNA with a first-stand cDNA synthesis kit (Amersham Pharmacia Biotechnology, Piscataway, NJ) according to the manufacturer's recommendations. The sequences of PCR primers that amplify human but not mouse genes are listed in Supplementary Table 1. PCR was performed with TaKaRa recombinant Taq (Takara Shuzo, Kyoto, Japan) for 30 cycles, with each cycle consisting of 94°C for 30 s, 62°C or 65°C for 30 s, and 72°C for 20 s, with an additional 10-min incubation at 72°C after completion of the last cycle.

Immunohistochemical and Immunocytochemical Analysis

Immunohistochemical analysis was performed as previously described (Mori *et al.*, 2005). Briefly, the sections were incubated for 1 h at room temperature with mouse mAb against vimentin (Cone V9, DakoCytomation, Fort Collins, CO). After washing in PBS, sections were incubated with horseradish peroxidase-conjugated rabbit anti-mouse immunoglobulin, diluted, and washed in cold PBS. Staining was developed by using a solution containing diaminobenzidine and 0.01% H_2O_2 in 0.05% M Tris-HCl buffer, pH 6.7. Slides were counterstained with hematoxylin. In the cases of fluorescence, frozen sections fixed with 4% PFA were used. The antibodies against human dystrophin (NCL-DYS3; Novocastra, Newcastle upon Tyne, United Kingdom) or anti-human nuclei mouse mAb (clone 235-1, Chemicon, Temecula, CA) was used as a first antibody, and goat anti-mouse IgG conjugated with Alexa Fluor 488 or goat anti-mouse IgG antibody conjugated with Alexa Fluor 546 (Molecular Probes, Eugene, OR) was used as a second antibody.

Immunocytochemical analysis was performed as previously described (Mori *et al.*, 2005), with antibodies to skeletal myosin (Sigma, St. Louis, MO; product no. M 4276), MF20 (which reacts with all sarcomere myosin in striated muscles, Developmental Studies Hybridoma Bank, University of Iowa, IA), α-sarcomeric actin (Sigma, product no. A 7811), and desmin (Bio-Science Products, Bern, Switzerland; no. 010031, clone: D9) in PBS containing 1% bovine serum albumin. As a methodological control, the primary antibody was omitted. In the cases of fluorescence, slides were incubated with Alexa Fluor 546–conjugated goat anti-mouse IgG antibody.

Western Blotting

Western blot analysis was performed as previously described (Mori *et al.*, 2005). Blots were incubated with primary antibodies (desmin, myogenin [Clone F5D, Santa Cruz Biotechnology], and dystrophin [NCL-DYSA, Novocastra]) for 1–2 h at room temperature. After washing three times in the blocking buffer, blots were incubated for 30 min with a horseradish peroxidase–conjugated secondary antibody (0.04 μg/ml) directed against the primary antibody. The blots were developed with enhanced chemiluminescence substrate according to the manufacturer's instructions.

Fusion Assay

EM-E6/E7/hTERT-2 cells (2500/cm^2) or EGFP-labeled EM-E6/E7/hTERT-2 cells (2500/cm^2) were cocultured with C2C12 myoblasts (2500/cm^2) for 2 d in DMEM supplemented with 10% FBS and then cultured for 7 additional days in DMEM with 2% HS to promote myotube formation. The cultures were fixed in 4% paraformaldehyde and stained with a mouse anti-human nuclei IgG1 mAb and the mouse anti-human dystrophin IgG2a mAb (or anti-myosin heavy chain IgG2b mAb MF-20). The cells were visualized with appropriate Alexa-fluor–conjugated goat anti-mouse IgG1 and IgG2a (or IgG2b) secondary antibodies (Molecular Probes). Total cell nuclei were stained with DAPI (4′,6-diamidino-2-phenylindole).

In Vivo Cell Implantation

Six- to 8-wk-old NOD/Shi-scid/IL-2 receptor −/− (NOG, CREA, Shizuoka, Japan) mice and 6- to 8-wk-old mdx-scid mice were implanted with EM-E6/E7/hTERT-2 cells and menstrual blood–derived cells in seven independent experiments. The cells (2×10^7) were suspended in PBS in a total volume of 100 μl and were directly injected into the right thigh muscle of NOG mice or mdx-scid mice. The mice were examined 3 wk after cell implantation, and the right thigh muscle was analyzed for human vimentin and dystrophin by immunohistochemistry. The antibodies to vimentin and dystrophin (NCL-DYS3) react with human vimentin and dystrophin-equivalent protein, but not murine protein.

RESULTS

Surface Marker Expression of Endometrium-derived Cells

We investigated myogenic differentiation of primary cells without gene introduction from menstrual blood, because menstrual blood on the first day of the period is considered to include endometrial tissue. We successfully cultured a large number of primary cells from menstrual blood. Menstrual blood–derived cells showed at least two morphologically different cell groups: small spindle-like cells and large stick-like cells, regarded as being passage day (PD) 1 or 2 (Figure 1, A and B, respectively). Surface markers of the menstrual blood–derived cells were evaluated by flow cytometric analysis. Surface markers of EM-E6/E7/hTERT-2 cells (Figure 1C) and menstrual blood–derived cells (Figure 1D) were evaluated by flow cytometric analysis (Figure 1E). In these experiments, the cells were cultured in the absence of any inductive stimuli. EM-E6/E7/hTERT-2 cells were positive for CD13, CD29 (integrin β1), CD44 (Pgp-1/ly24), CD54, CD55, CD59, CD73, and CD90 (Thy-1), implying that EM-E6/E7/hTERT-2 cells expressed mesenchymal cell–related antigens in our experimental setting. Menstrual blood–derived cells were positive for CD13, CD29, CD44, CD54, CD55, CD59, CD73, CD90, and CD105, implying that prolif-

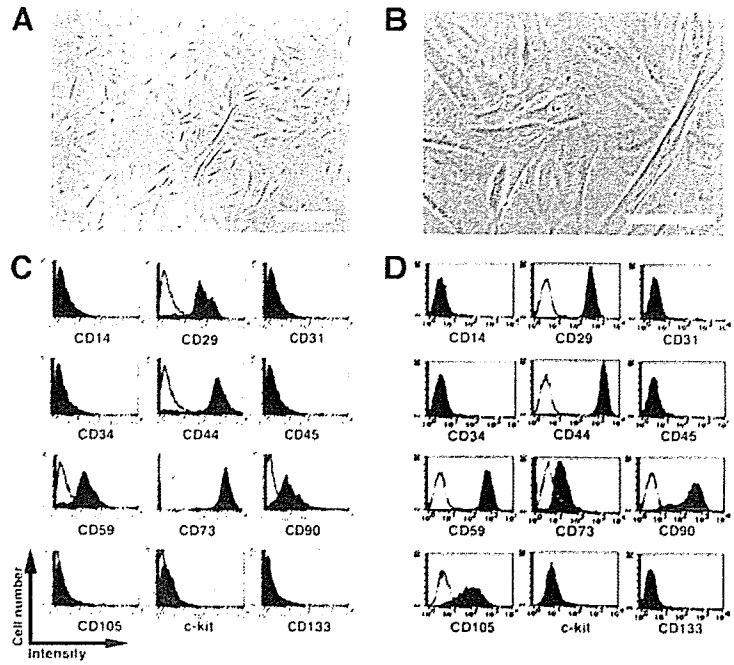

E

Surface marker	EM-E6/E7/ hTERT-2 cells	Menstrual blood cells	Surface marker	EM-E6/E7/ hTERT-2 cells	Menstrual blood cells
CD13	+	++	CD55	++	++
CD14	-	-	CD59	++	+++
CD29	++	+++	CD73	+++	+
CD31	-	-	CD90	++	+++
CD34	-	-	CD105	-	++
CD44	+++	+++	c-kit	-	-
CD45	-	-	CD133	-	-
CD50	-	-	HLA-ABC	++	++
CD54	+	++	HLA-DR	-	-

Figure 1. Surface marker expression of endometrium-derived cells. (A and B) Morphology of menstrual blood–derived cells, regarded as being PD 1 or 2. Scale bars, 200 μm (A), 100 μm (B). (C and D) Flow cytometric analysis of cell surface markers of EM-E6/E7/hTERT-2 cells (C) and menstrual blood–derived cells (D). (E) Further phenotypic analysis in EM-E6/E7/hTERT-2 cells and menstrual blood–derived cells are summarized. Peak intensity was estimated in comparison with isotype controls. +++, strongly positive (>100 times the isotype control); ++, moderately positive (<100 times but more than 10 times the isotype control), weakly positive (<10 times but more than twice the isotype control), −, negative (less than twice the isotype control).

erated and propagated cells express mesenchymal cell-related cell surface markers. Unlike EM-E6/E7/hTERT-2 cells, the menstrual blood–derived adherent cells were positive for CD105. EM-E6/E7/hTERT-2 cells and menstrual blood–derived cells expressed neither hematopoietic lineage markers, such as CD34, nor monocyte-macrophage antigens such as CD14 (a marker for macrophage and dendritic cells), or CD45 (leukocyte common antigen). The lack of expression of CD14, CD34, or CD45 suggests that EM-E6/E7/hTERT-2 cells and the menstrual blood–derived cell culture in the present study is depleted of hematopoietic cells. The cells were also negative for expression of CD31 (PECAM-1), CD50, c-kit, and CD133. The cell population was positive for HLA-ABC, but not for HLA-DR. These results demonstrate that almost all cells derived from endometrium are of mesenchymal origin or stromal origin.

Implanted Endometrium-derived Cells Induce De Novo Myogenesis in Immunodeficient NOG Mice

EM-E6/E7/hTERT-2 cells originate from the endometrial gland and are considered as endometrial progenitor cells or bipotential cells capable of differentiating into both glandular epithelial cells and endometrial stromal cells (Kyo *et al.*, 2003). To determine whether EM-E6/E7/hTERT-2 cells and menstrual blood–derived cells generate complete endometrial structure in vivo, like endometriosis, the cells without any treatment or induction were injected into the right thigh muscle of immunodeficient NOG mice. PBS without cells was injected into the left thigh muscles as a control. We failed to detect any endometrial structure in the cell-injected site. Immunohistochemical analysis using an antibody specific to human vimentin, an intermediate filament associated with a mesenchymal cell, revealed that the injected EM-E6/E7/hTERT-2 cells (Figure 2, A–F) or menstrual blood–derived cells (Figure 2, G–L) extensively migrated or infiltrated between muscular fibers (Figure 2, arrowheads). To investigate if the donor cells between muscular fibers occur as a result of cell migration, we performed a time-course analysis of implanted cells, as probed by human-specific antibody to vimentin (Supplementary Figure 1). Donor cells at 3 h after implantation are observed at the injection site, which is considered to be due to just injection of cells. Cells at 1–3 wk after implantation are detected between myocytes in the muscle bundle or muscular fascicle as well as in the interstitial tissue, implying that the donor cells between myotubes result from cell migration. Interestingly, some of the vimentin-positive implanted cells exhibited round-shaped structure (Figure 2, D, F, and J, arrows), suggesting that endometrium-derived cells are capable of differentiating into myoblasts/myotubes, and can contribute to skeletal muscle repair in patients suffering from genetic disorders such as DMD, similar to previous reports for marrow stromal cells (Dezawa *et al.*, 2005) and synovial membrane cells (De Bari *et al.*, 2003).

balt2/zmk-mbc/zmk-mbc/zmk00507/zmk8034-07z | xppws | S=1 | 2/26/07 | 6:51 | 4/Color Figure(s): F1–6 | Art: 3198875 | Input-cip

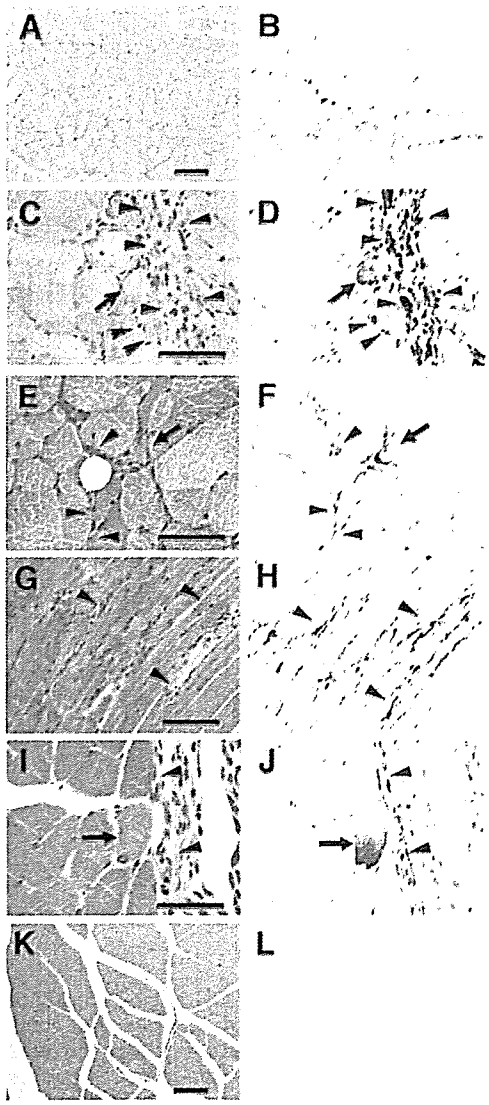

Figure 2. Implantation of endometrium-derived cells-derived cells into the muscle of NOG mice. EM-E6/E7/hTERT-2 cells (A–F) or menstrual blood–derived cells (G–J) cultured in absence of any stimuli were directly injected into the right thigh muscle of NOG mice. Immunohistochemical analysis was performed using antibody that reacts to human vimentin but not to murine vimentin. (A, C, E, G, I, and K) hematoxylin and eosin stain (HE; B, D, F, H, J, and L) immunohistochemistry. Note that vimentin-positive EM-E6/E7/hTERT-2 cells and menstrual blood–derived cells with a spindle morphology (C–J, arrowheads) extensively migrated into muscular bundles at 3 wk after injection, and some of the injected cells exhibited round structure (D, F, and J, arrows). Isotype mouse IgG1 served as a negative control (L). Scale bars, 100 μm (A, B, K, and L), 50 μm (C–F, I, and J), 90 μm (G and H).

Induction of Myogenic Differentiation in Endometrial Progenitor Cells In Vitro

EM-E6/E7/hTERT-2 cells at 2 wk (cultured in the DMEM supplemented with 20% FBS) after exposure to different concentrations (5, 10, and 100 μM) of 5-azacytidine were analyzed by immunostaining using anti-desmin antibody (Figure 3, A–F). The number of desmin-positive cells was significantly higher in experimental groups with 5 or 10 μM 5-azacytidine than in untreated control groups ($p < 0.05$). To investigate whether EM-E6/E7/hTERT-2 cells are capable of differentiating into skeletal muscle cells in vitro, the cells were exposed to 5 μM 5-azacytidine for 24 h and then subsequently cultured in the DMEM supplemented with 2% HS (Figure 3, G–J) or serum-free ITS for up to 21 d (Figure 3K). Skeletal myoblastic differentiation of the cells was analyzed by evaluating expression of MyoD, Myf5, desmin, myogenin, MyHC-IIx/d, and dystrophin by RT-PCR. The MyoD, desmin, myogenin, and dystrophin genes were constitutively expressed, but MyHC-IIx/d and Myf5 genes were not. The decline of MyoD was observed in both the 2% HS (Figure 3, G and H) and the serum-free ITS (Figure 3K). The expression of MyHC, as determined by RT-PCR and immunocytochemistry, significantly increased with 2% HS (Figure 3, G–J) and serum-free ITS (Figure 3K). Immunocytochemical analysis indicated that α-sarcomeric actin (Figure 3I) and MyHC (Figure 3J) were detected in the cells incubated with 2% HS for 21 d.

In Vitro Myogenic Differentiation of Menstrual Blood-derived Cells

Menstrual blood–derived cells at 3 wk (cultured in DMEM supplemented with 20% FBS) after exposure to different concentrations (5, 10, and 100 μM) of 5-azacytidine were analyzed by immunostaining using anti-desmin antibody (data not shown). The number of desmin-positive cells was significantly higher in experimental groups with 5 or 10 μM 5-azacytidine than with 100 μM 5-azacytidine; for further in vitro experiments, the menstrual blood–derived cells were exposed to 5 μM 5-azacytidine for 24 h and then subsequently cultured in DMEM supplemented with low serum (2% HS) or serum-free ITS for up to 21 d (Figure 4). Myogenic potential of human menstrual blood–derived cells was analyzed by evaluating the expression of Myf5, MyoD, desmin, myogenin, MyHC-IIx/d, and dystrophin by RT-PCR. MyoD, desmin, and dystrophin genes were constitutively expressed in menstrual blood–derived cells, but MyHC-IIx/d and Myf5 were not (Figure 4A). For cells treated with 2% HS or serum-free ITS, the mRNA level of desmin and myogenin significantly increased after 3 d, and desmin steadily increased until day 21 (Figure 4, C and D). MyHC-IIx/d started to be expressed at a low level at day 21 of induction (Figure 4C). We then analyzed desmin expression by immunocytochemistry. Menstrual blood–derived cells were exposed to 5 μM 5-azacytidine for 24 h and then subsequently cultured in DMEM supplemented with 20% FBS for up to 2 wk. Desmin was readily detected in colonies of the menstrual blood–derived cells (Figure 4B). Western blot analysis indicated that desmin, myogenin, and dystrophin were highly expressed in the cells incubated for 3 wk (Figure 4, E–G). These results suggest that menstrual blood–derived cells are, like the EM-E6/E7/hTERT-2 cells, able to differentiate into skeletal muscle.

Regeneration of Dystrophin by Cell Implantation in the DMD Model mdx-scid Mouse

To investigate whether human EM-E6/E7/hTERT-2 cells and menstrual blood–derived cells can generate muscle tissue in vivo, cells without any treatment or induction were implanted directly into the right thigh muscles of mdx-scid mice (Supplementary Figure 2). The left thigh muscles were injected with PBS as an internal control. After 3 wk, myotubes in the muscle tissues injected with human EM-E6/E7/hTERT-2 cells and menstrual blood–derived cells expressed human dystrophin as a cluster (Figure 5, A, C, and D, EM-